AN ABSTRACT OF THE THESIS OF

THOMAS WARD OSBORN III (Name) for the MASTER OF SCIENCE (Degree)

in CHEMISTRY (Major) presented on August 13, 1968 (Date)

Title: SODIUM AND MANGANESE HOMOGENEITY IN CHONDRITIC METEORITES

Abstract approved: Redacted for Privacy
Roman A. Schmitt

Four to six one-gram specimens separated by a distance of several inches were obtained from each of 23 large chondritic meteorites (approximately 1 kg each) representing the olivine bronzite (H5), olivine hypersthene (L6) and enstatite (E5) classifications. Each specimen was analyzed for Na and Mn via instrumental neutron activation analysis to a precision of about 1.5% using the 2.75 Mev and 0.84 Mev photopeaks for Na and Mn, respectively.

The olivine bronzite (H5) falls were found to exhibit a Mn homogeneity dispersion range of 3.9% to 1.7% for the large individual meteorites; Na dispersion range was 5.2% to 4.9%. One group of olivine bronzite (H5) finds consisting of five large meteorite fragments exhibited a Mn dispersion range of 0.8% to 2.7%; Na dispersion range was 1.8% to 4.7%. Another group of olivine bronzite (H5) finds consisting of four large pieces showed a Mn dispersion range from 3.8% to 17%; Na dispersion range, 3.8% to 31%. The olivine

hypersthene (L6) falls showed a Mn dispersion of 1.4% to 3.4%; Na dispersion, 2.0% to 7.1%. The olivine hypersthene finds showed a Mn dispersion range of 2.5% to 5.3%; Na dispersion range, 1.5% to 7.6%. The single enstatite find showed a relative dispersion of 45% for Mn and 28% for Na.

It was found that the olivine bronzite (H5) group may be divided into two subgroups on the basis of abundances and the homogeneity of Mn.

No significant correlation between the lithophilic elements Mn and Ha was established.

It was found that terrestrial fractionation presumably by leaching, may occur causing a significant depletion in Na. Manganese does not exhibit large depletion factors. The relative dispersion of both sodium and manganese are shown to increase by a factor of about two for finds compared to falls.

It is suggested that for some of olivine-hypersthene falls an Mn concentration gradient may be present.

Assuming chondrites represent the initial accretion products from the primitive solar nebula in the asteroidal volume of the solar system, the dispersion of Mn and Na suggest that the nebula was homogeneous within 1 to 4 percent.

Sodium and Manganese Homogeneity in Chondritic Meteorites

by

Thomas Ward Osborn III

A THESIS

submitted to

Oregon State University

in partial fulfillment of
the requirements for the
degree of

Master of Science

June 1969

APPROVED:

Redacted for Privacy

Associate Professor of Chemistry
in charge of major

Redacted for Privacy

Head of Department of Chemistry

Redacted for Privacy

Dean of Graduate School

Date thesis is presented August 13, 1968

Typed by Marion F. Palmateer for Thomas W. Osborn

ACKNOWLEDGMENTS

The author wishes to express his gratitude to Dr. Roman A. Schmitt, for his help, guidance, encouragement, and for a N. A. S. A. research assistantship throughout the course of this work.

Appreciation is also due Dr. Thomas Linn and Dr. Walter Loveland for their many helpful suggestions.

Finally the author wishes to thank his parents, Renata and Thomas Osborn, Jr., for their many contributions to his education.

TABLE OF CONTENTS

LIST OF TABLES

LIST OF FIGURES

SODIUM AND MANGANESE HOMOGENEITY IN CHONDRITIC METEORITES

INTRODUCTION

In recent years great interest has developed in the study of meteorites due primarily to the general agreement of solar abundances and the abundances of the chemical elements observed in chondritic meteorites. Studies on meteorites also yield vast amounts of information regarding the conditions of the primitive solar system, the formation of planets and subsequent cosmochemical fractionation processes which occurred in the accreted bodies. However, there exists only limited information on the homogeneity of these extraterrestial bodies which is absolutely essential in gaining a full picture of the accretion and subsequent cosmochemical fraction processes experienced by the parent bodies. Therefore, this study was undertaken as a preliminary study on the homogeneity of Na and Mn in chondritic meteorites with a precision of 1. 5% for determination of these two elements via instrumental neutron activation analysis.

The purposes of the study are given below:

1. To determine the homogeneity of Na and Mn in 26 large (> 1 kg) chondritic meteorites by sampling each meteorite in four to six positions (1 gm each) which were separated by several inches and analyzing each 1 gm specimen for Na and Mn via instrumental

neutron activation analysis (INAA).

2. To yield information which would aid in determining if the primary fractionation process in chondritic meteorites occurred in a preaccretion process or postaccretion process.

3. To establish any significant correlation in the sodium and manganese distributions.

4. To determine to what extent sodium and manganese had been leached during weathering and establish the degree of uniformity in the leaching process.

5. To provide a limited comparison between three of the chondritic subclasses: Enstatite, olivine bronzite, and olivine hypersthene.

6. To determine if in previous work significant sampling errors could have been present.

7. To determine if extended investigations along these lines would provide useful and pertinant data as to the origin and genetic history of meteorites.

HISTORICAL

Meteorites

Background

The general area of cosmochemistry and meteoritics is a new branch of chemistry which borrows methods and terminologies from many allied fields, in particular, physics and geology. Also there are many ideas which are unique to this field which the more conventional chemist may not be familiar with. Therefore, this section will be more comprehensive than in most theses so that the problem may be seen in perspective.

In 1802 an English chemist, Edward C. Howard, made a short systematic study on the internal structure of stony meteorites. His primary observation was that there were "abundant small bodies, some perfectly globular, others elongated or elliptical" (36). The size of these small bodies ranged from that of a pin head to that of a small pea, with a color range from gray to brown.

When Howard made his observation the idea that meteorites were extraterrestial was considered to be a complete hoax. In 1803, the French village L'Aigle experienced a massive shower of rocks which the physicist Jean Baptiste Biot confirmed in a report to the Académie des Sciences. After Biot's famous report museums

collected meteorites as the only extraterrestrial fragments to which man had direct access. Then in 1864 the German mineralogist, Gustav Rose, named the class of stony meteorites chondrites in accordance with their unique internal structure. The small rounded inclusions in the meteorites were called chondrules after the Greek word Chondros for "grain of seed." There were isolated individuals from then up to the 1950's that made investigations concerning meteorites. With the advent of the space age great interest has developed in meteorites as a clue to the origin of the solar system and the universe.

Finds, Falls and Orbits

A meteorite which was actually seen to fall and subsequently picked up a short time later is called a "fall" in contrast to a "find" which is recognized as extraterrestrial on the basis of chemical composition, mineralogy, and structure. The Hey Catalogue (12) gives the following statistics concerning falls and finds.

Table 1. Classification of falls.

	Falls	%	Finds	%	Total	%
Irons	42	6	503	59	545	35
Stony-irons	12	2	55	6	67	4
Stones	628	92	304	35	932	61
Total	682	100	862	100	1544	100

This short table shows that stones are by far the most abundant among the observed falls. They are less abundant among the finds since they are easily overlooked as a meteorite in contrast to the irons.

Meteorites have been found on all continents but vary greatly in the number and type recovered. It is presumed that the recovery and recognition of meteorites is closely related to the population density, the educational and cultural level of the area. Meteorites are most often found on plains in contrast to mountainous regions. The relative number of the irons recovered to stones recovered varies greatly for different continents. In North America 363 stones have been found and 330 irons while in Europe 42 irons and 300 stones have been found. This is taken to be indicative of which societies had the skill of metal working. The following chart categorizes the stones and irons into the number found in each continent.

Table 2. Geographic distribution of meteorites.

	North America	South America	Australia	Europe	Asia	Africa
Irons	330	59	61	42	47	35
Stones	363	37	40	300	200	65

There are also distinct variations noted for the observed falls of meteorites as to months and time of day observed. The monthly

variations may reflect that more observers are present in the western hemisphere during the summer months or that during certain periods the earth may pass through a region of space more densely populated with meteoritic material. The distinct hourly variation reflects two aspects:

1. The number of observers present.

2. The fact that all meteorites reaching the earth between noon and midnight are necessarily traveling in the same direction as the earth. Thus it appears that the majority are moving in the same direction as the earth in its motion around the sun.

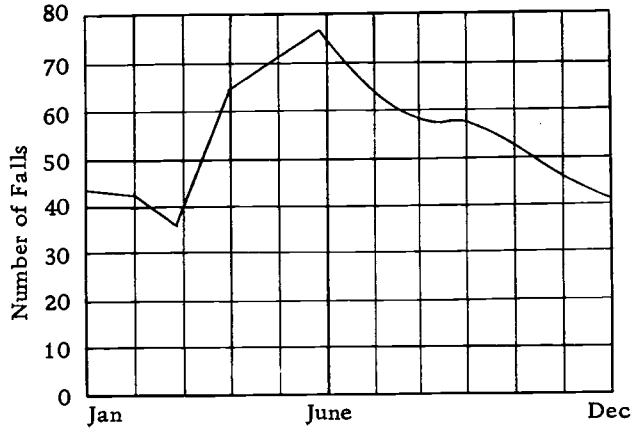

Figure 1. Monthly variation in the number of meteorite fall, Mason (21).

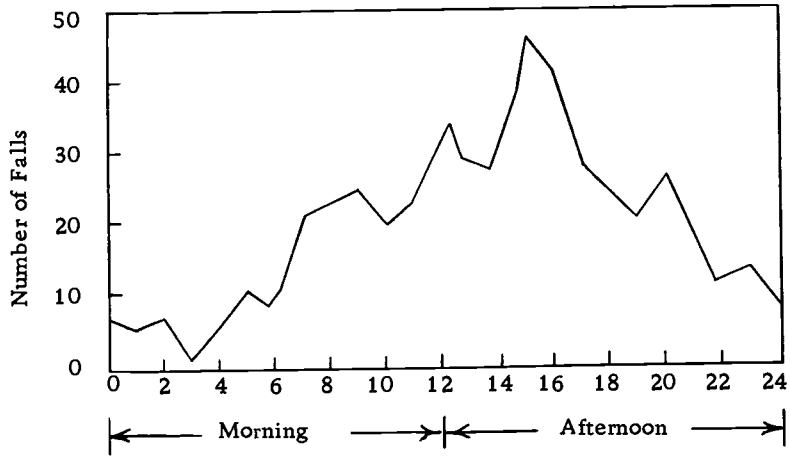

Figure 2. Hourly variation in the number of meteorite falls, Mason (21).

Most experts agree that most meteorites come from the asteroid belt rather than from the moon. The orbits and geocentric velocities of the stony meteorites resemble those of the Apollo asteroids but disagree greatly with the orbits and velocities calculated for lunar ejections (9). It has also been generally agreed that meteorites travel in elliptical orbits and evidence of this was presented by Krinov (13). The Pribram chondrite which fell April 7, 1959, was the only meteorite photographed adequately during its descent to determine its orbit. The calculations showed that this

meteorite was traveling in an eliptical orbit originating in the asteroid belt.

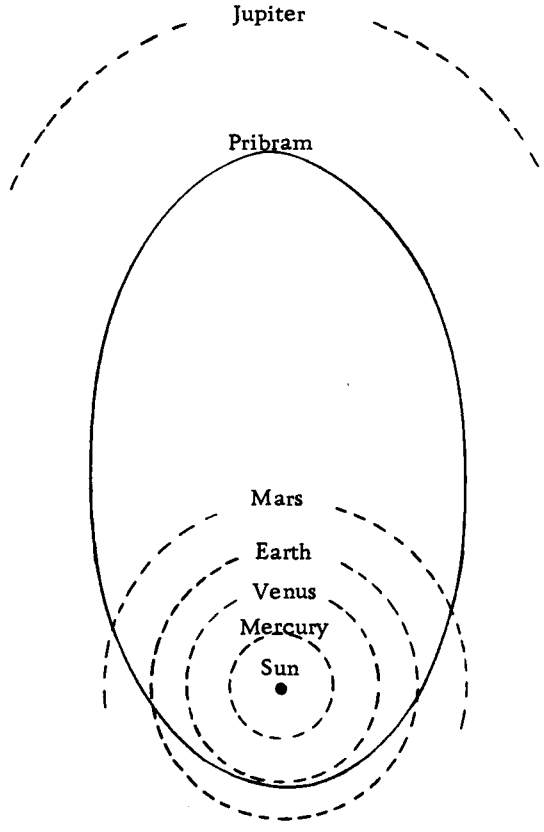

Figure 3. Orbit of Pribram Meteorite, Mason (21).

General Classifications and Ages

Meteorites may be classified into three broad categories:

1. Aerolites or stones which are mainly composed of silicate minerals with some nickel-iron alloy. The stones are then further classified into chondrites or achondrites depending upon the presence

or absence of condrules. The condrites are further divided into carbonaceous, olivine bronzite, olivine-hypersthene and enstatites on the basis of chemical composition and mineralogy.

2. Siderolites or stony-irons which are about 50% metallic and 50% siliciate minerals.

3. Siderites or irons which consist primarily of nickel-iron..

There are numerous methods for the determination of meteorite ages which involve the use of radioactivity or isotope ratios. The various methods imply ages or dates for different processes to which the meteorites have been subjected.

Patterson in 1956 (21) showed that the well known lead isotope ratio method could also be applied to meteorites. His results gave the age of 4.55 $\pm$ 0.07 aeons (1 aeon is 10^9 years). This age is generally assumed to be the accretion and melting age of the parent body. Helium from uranium decay is also used for dating meteorites.

Potassium-argon ages for stony meteorites were first determined in 1951; since then, many age determinations via this method have been made. The ages generally run from 0.5 to 4.5 aeons with most of the values falling between 4.0 and 4.5 aeons. It is assumed that the lower ages are a result of argon loss and that the ages give the time of crystallization of the meteorites.

The radiogenic methods of dating meteorites give a set of ages which are reasonably in line with the age of the earth. Thus the

earth and meteorites were formed about the same time and give reasonable agreement with the solar system's age.

Cosmic rays interact with nuclei to cause spallation reactions and the measure of the products are assumed to give the length of time the meteorite was exposed to a flux of cosmic radiation, i. e., the length of time from the parent body break-up to the meteorite's arrival on earth. Most bronzite chondrites lie in a single cluster around 4 my. with the hypersthene chondrites cluster at 3, 7-13, and 16-31 my. Anders (3) has assumed that each of these clusters indicate separate breakups.

Another method of dating involves the use of short lived radioactive isotopes on the order of 100 million year $t_{1/2}$ (half-life). This method is assumed to give the age of a body from the time of nucleosynthesis to its accretion provided there has been no subsequent loss of decay products. The method involves the I^{129}/Xe^{129} ratio which involves the 16. 4 my. $t_{1/2}$ of I^{129}. It has been calculated (9) that the formation of Richardton occurred 50 my. after the end of the nucleosynthesis period.

Reynolds also found abundances of Xe^{124} and Xe^{126} to be three times more abundant in chondrules than in terrestrial xenon. The excess xenon ratios can be made only by proton or alpha particle reactions, thus this would date the formation of chondrules to be before accretion (28).

Mineralogy

The minerals found in meteorites are distinctly igneous in nature, they also show distinct evidence of being subjected to metamorphic processes causing a more uniform composition in the elemental distribution. Metamorphism also is evidenced in the recrystallization and obliteration of earlier structure, the chondrules.

Different elements have different tendencies to associate themselves with other elements. Goldschmitt classified these into four groups:

1. Siderophilic elements are those associating themselves with iron.

2. Chalchophilic elements are those associating themselves with sulfur.

3. Lithophilic elements are those associating themselves with the silicate phase.

4. Atmophilic elements are those associating themselves with gaseous phase.

Table 3. Geochemical classification of the elements, Goldschmidt, (11).

Siderophile	Chalcophile	Lithophile	Atmophile
Fe Co Ni	Cu Ag	Li Na K Rb Cs	H N (C)(O)
Ru Rh Pd	Zn Cd Hg	Be Mg Ca Sr Ba	Inert gases
Os Ir Pt	Ga In Tl	B Al Sc Y	
Au Re Mo	(Ge)(Sn)Rb	Rare earths	
Ge Sn	As Sb Bi	(C)Si Ti Zr Hf Th	
C P	S Se Te	(P) V Nb Ta	
(Pb) (As)(W)	(Fe)(Mo)(Cr)	O Cr W U	
		(H) F Cl Br I	
		(Tl)(Ga)(Ge)	
		(Fe) Mn	

Of these elements the normally lithophilic Ca, Ti, Cr and Mn are considered chalcophilic in meteorites showing a very high degree of reduction (20).

The following is a list of minerals found in meteorites and their chemical formulas (Table 4).

Chondrites and Their Chemical Composition

Chondrites are not only the most abundant meteorites but perhaps the most important in reaching a basic understanding of the origin of meteorites and the solar system. "The real test of a theory of meteorites is its ability to account for chondrites" (3).

Table 4. Major minerals in meteorites, Wood (37).

Mineral	Composition	Crystal System
	Silicates	
Olivine	$(Mg_{1-f}Fe_f)_2SiO_4$	Orthorhombic
Forsterite	$f \sim 0$	"
Fayalite	$f \sim 1$	"
Orthopyroxene	$(Mg_{1-f}Fe_f)SiO_3$	Orthorhombic
Enstatite	$f < 0.1$	"
Bronzite	$0.1 < f < 0.2$	"
Hypersthene	$f > 0.2$	"
Clinopyroxene (Including augite, pigeonite, diopside, clinohypersthene, etc.)	General formula: $(Ca, Na, Mg)(Mg, Fe^{++}, Mn, Al, Fe^{+++})(Al, Si)SiO_6$	Monoclinic
Plagioclase Feldspar	$(NaAlSi_3O_8)_{1-An}CaAl_2Si_2O_8)_{An}$	Triclinic
Albite	$An < 0.1$	"
Oligoclase	$0.1 < An < 0.3$	"
Andesine	$0.3 < An < 0.5$	"
Labradorite	$0.5 < An < 0.7$	"
Bytownite	$0.7 < An < 0.9$	"
Anorthite	$0.9 < An$	"
	Non-silicates	
Nickel-iron		Cubic
Kamacite	< 8% Ni	" (b. c. c.)
Taenite	>20% Ni	" (f. c. c.)
Troilite	$FeS_x (x \sim 1)$	Hexagonal
Chromite	$FeCr_2O_4$	Cubic
Schreibersite	$(Fe, Ni)_3P$	Tetragonal

The initial classification of chondritic meteorites was made by Rose in 1863 and in 1872 Tschermak extended Rose's classification on the basis of color and structure. Later Brezina in 1904 extended the classification again until 31 distinct groups were recognized. The Rose-Tschermak-Brezina classification is still widely used but is rapidly being replaced by other systems.

Prior in 1920 proposed a classification based on the chemical and mineralogical composition distinguishing three groups.

1. Enstatite chondrites which consist of the orthopyroxene mineral enstatite ($MgSiO_3$) which is almost completely free of iron. Large amounts of nickel-iron, up to 25% which is lacking in nickel (Fe/Ni = 13), troilite (FeS) and some oligoclase (10 - 30% Ca $Al_2Si_2O_8$ + 90-70% Na $AlSi_3O_8$) is also present.

2. Olivine-bronzite or bronzite chondrites which consist of approximately equal portions of bronzite (10 - 20% $FeSiO_3$ + 90 - 80% $MgSiO_3$) and olivine ($(Mg, Fe)_2SiO_4$) and with smaller amounts of oligoclase and nickel-iron. The nickel-iron is more abundant in nickel than are the enstatites with MgO/FeO $\approx$ 5.

3. Olivine-hypersthene or hypersthene are similar in structure and composition to the olivine-bronzite except that the nickel is more abundant in the nickel-iron phase with Fe/Ni $\approx$ 7-3 and the ferro-magnesium minerals are more abundant in FeO where MgO/FeO = 4 - .2..5.

Prior established certain chemical and mineralogical relationships within the chondrites. These relations are expressed as Prior's Rules (21):

1. The smaller the amount of nickel-iron in a chondrite the higher the Ni/Fe ratio in the metal phase.

2. The smaller the amount of nickel-iron in a chondrite the higher the FeO/MgO ratio in ferromagnesium silicate minerals.

Although Prior's classification was described in mineralogical terms the classification itself is essentially chemical establishing three criteria for chondrite classification:

1. The MgO/FeO ratio in the bulk analysis.

2. The MgO/FeO ratio in the silicate phase insoluble in HCL (the pyroxene minerals).

3. The amount of nickel-iron and the Fe/Ni ratio.

Mason (21) has extended Prior's classification by the subdivision of some of the olivine-hypersthene meteorites into two new classes; namely, the olivine-pigeonite and the carbonaceous chondrites. The two new classes were very small containing 12 and 17 meteorites, respectively. Mason has since rejected the pigeonite classification and now calls them Type III Carbonaceous.

The chemical composition of a given subgroup is for the most part quite similar showing a continuous variation of values but when comparison between subclasses are made great differences may

become evident. Such a difference was noted by Urey and Craig in 1953 (34) in the comparison of total iron content. The superior analyses of Urey and Craig are plotted but only using the falls. It is evident that each of the five groups occupy a region of specific composition and there is essentially no overlap of the different groups.

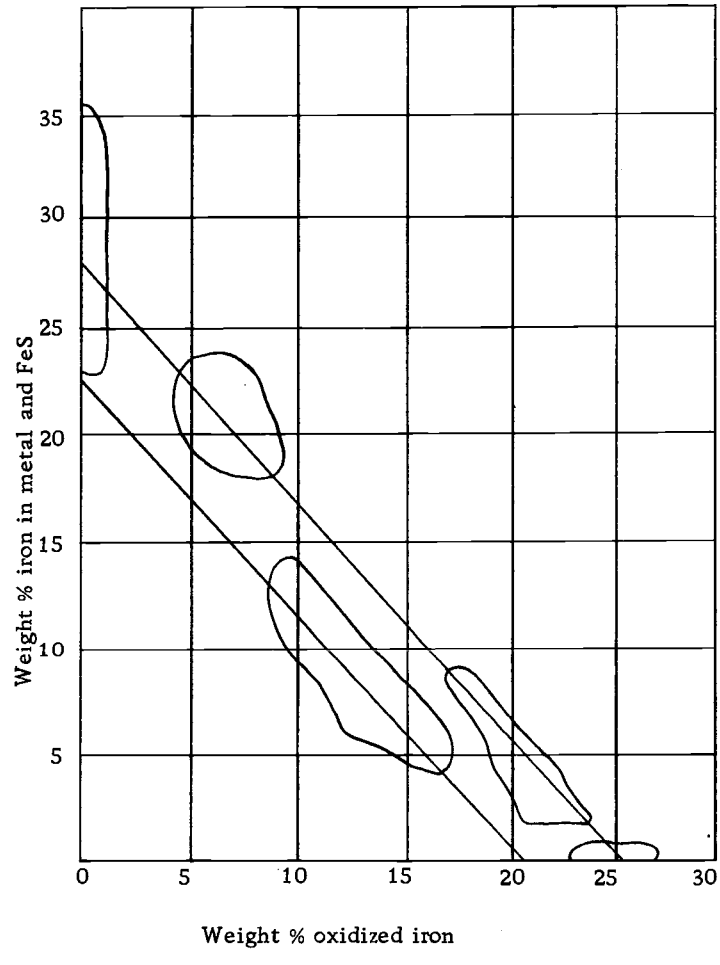

Figure 4. Classification by degree of oxidation (33).

The lines at 45° represent constant iron content. The top line corresponds to about 28% total iron and the lower line corresponds to about 22% total iron. Urey and Craig designated these groups the High (H) and Low (L) groups. There is a very definite grouping apparent between the iron contents: All olivine-hypersthene are L type while all carbonaceous, and olivine bronzite belong to the H type. Wood has suggested that the enstatites which show a considerable spread be considered in an HH group for those that have a much higher iron content.

Van Schmus and Wood (36) have enlarged and extended the grouping of Urey and Craig in the following system.

1. The weight ratio of total FeO/SiO_2 in the bulk analysis. This is essentially the way Urey and Craig present the differences in iron content.

2. The weight ratio of SiO_2/MgO in the bulk analysis which can be used to distinguish three chemical groups: E (enstatite), C (carbonaceous) and the ordinary chondrites (H, L, LL).

3. The molecular ratio $FeO/(FeO + MgO)$ in the olivine and pyroxene phases. It has been demonstrated (19) that for homogeneous olivine and pyroxenes the fayalite content of the olivine and the ferrosilite content of the pyroxene correlate with the bulk FeO content.

4. The Fe°/Fe ratio(metallic iron/total iron) expresses the degree of oxidation of the iron in the chondrites. For well

crystalized systems it is directly related to (1) and (3) above, by a material balance.

The characterics of the five recognized groups of the chondrites are given below following the outline of Van Schmus and Wood.

E. Group. This group is essentially the group that Mason called the enstatite group. It has unique mineralogy which is a reflection of this group's unique chemical composition. This group is distinguished from the other groups on the basis of its low degree of oxidation resulting in the highest Fe°/Fe ratios. Not only is the iron primarily in the metal but other elements: Ca, Mn and Cr may be present in the sulfide phases, and some Si is present in the metal phase. Decreasing iron content appears to correlate with the degree of recrystallization and, therefore, the inhomogeneity of iron may be related to secondary processes rather than primary in origin.

The principle mineral is enstatite which is nearly pure $MgSiO_3$. Olivine is normally absent but SiO_2 is often present in excess amounts as quartz or other metamorphic minerals. The metallic phase is entirely kamacite.

C Group. This group is classified by Type I, Type II, and Type III carbonaceous condrites. Most of the meteorites referred to by Mason as "olivine-pigeonite" are in the Type III class. The C group has a lower SiO_2/MgO ratio and they are very deficient in metallic iron. It has been suggested by Ringwood (27) that ordinary

chondrites were formed by the auto-reduction of highly oxidized carbon containing matter similar to Type I carbonaceous chondrites.

H Group. This group is identified by its bulk chemistry showing the highest Fe/SiO_2 ratios and the highest Fe°/Fe ratios indicating a low degree of oxidation. This group includes the bronzite and unequilibrated chondrites of the H group chemistry. The FeO content ranges from 7 - 12% but in contrast to the E group the calcium, chromium and manganese are present almost entirely as the oxides.

This group has homogeneous olivine and pyroxene and the low degree of oxidation is also exhibited in the low FeO/FeO + MgO ratios of the olivine and pyroxene. The vast majority of the H-group is recognized by the high fayalite (Fe_2SiO_4) content (16 - 20 mole %).

L and LL Groups. Both of these groups are distinguishable from the H group by a lower total iron content and higher degree of oxidation.

The LL group has a lower total iron content than the L group and even a higher degree of oxidation than the L group.

The presence of distinct clustering by the U-He age determinations have shown them to be sharply differentiated. The LL group had extensive out-gassing by the collision about 520 my. and the L group have a high gas age of about 4 Ae.

Van Schmus and Wood continue to subdivide the five chemical

classes into six petrological divisions (implied metamorphic) producing 30 possible types of which 20 are recognized.

The following two graphs illustrate how the divisions occur.

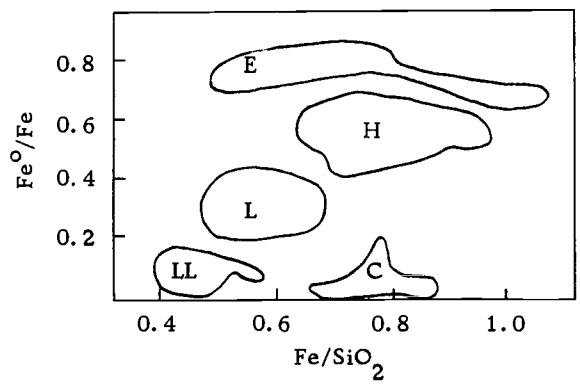

Figure 5. Chemical classification of meteorites.

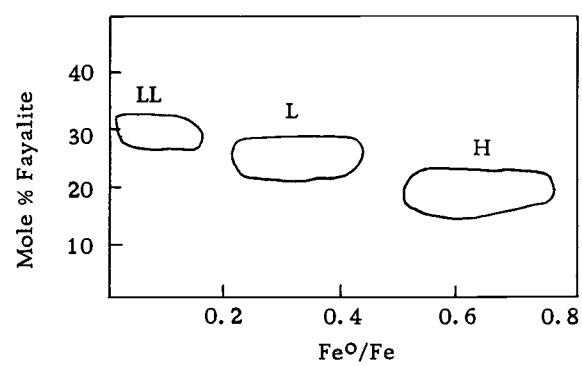

Figure 6. Chemical classification for ordinary meteorites (36).

A comparison of several important elements in chondrites, in the solar atmosphere and Hawaiian olivine basalt serves to help place the abundance of these elements in perspective. The chart is a simplified version of Woods (39).

Table 5. Relative abundances of elements.

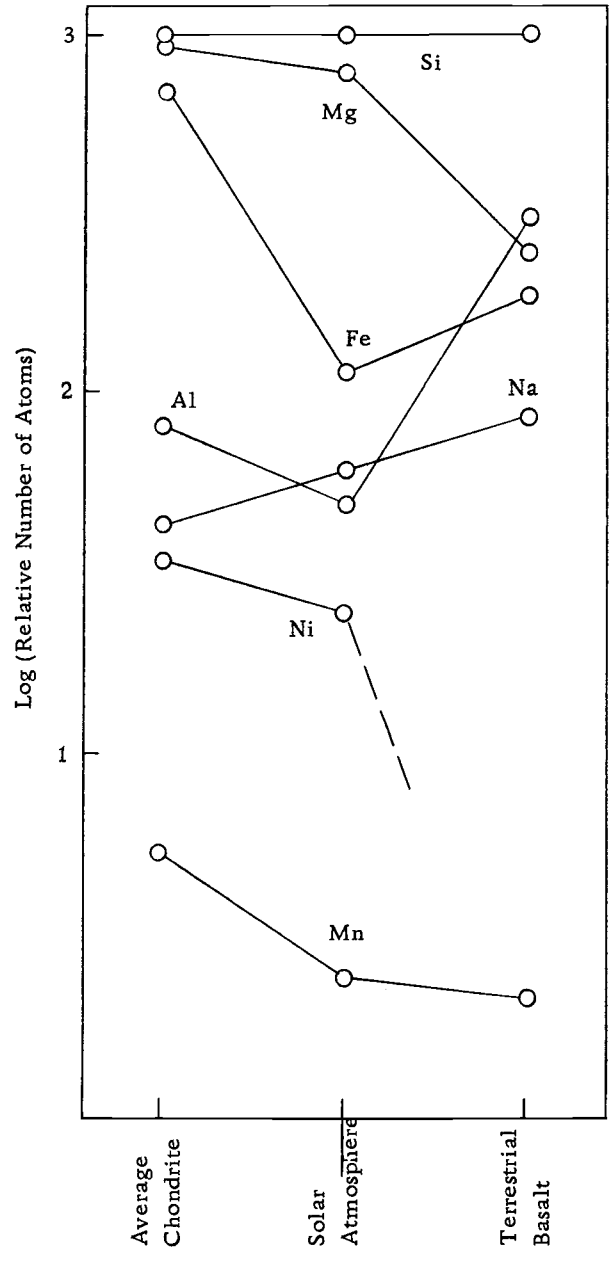

Another chart shows a more extensive comparison of elemental abundances of chondrites and the solar atmosphere to picture the similarity of the abundance patterns.

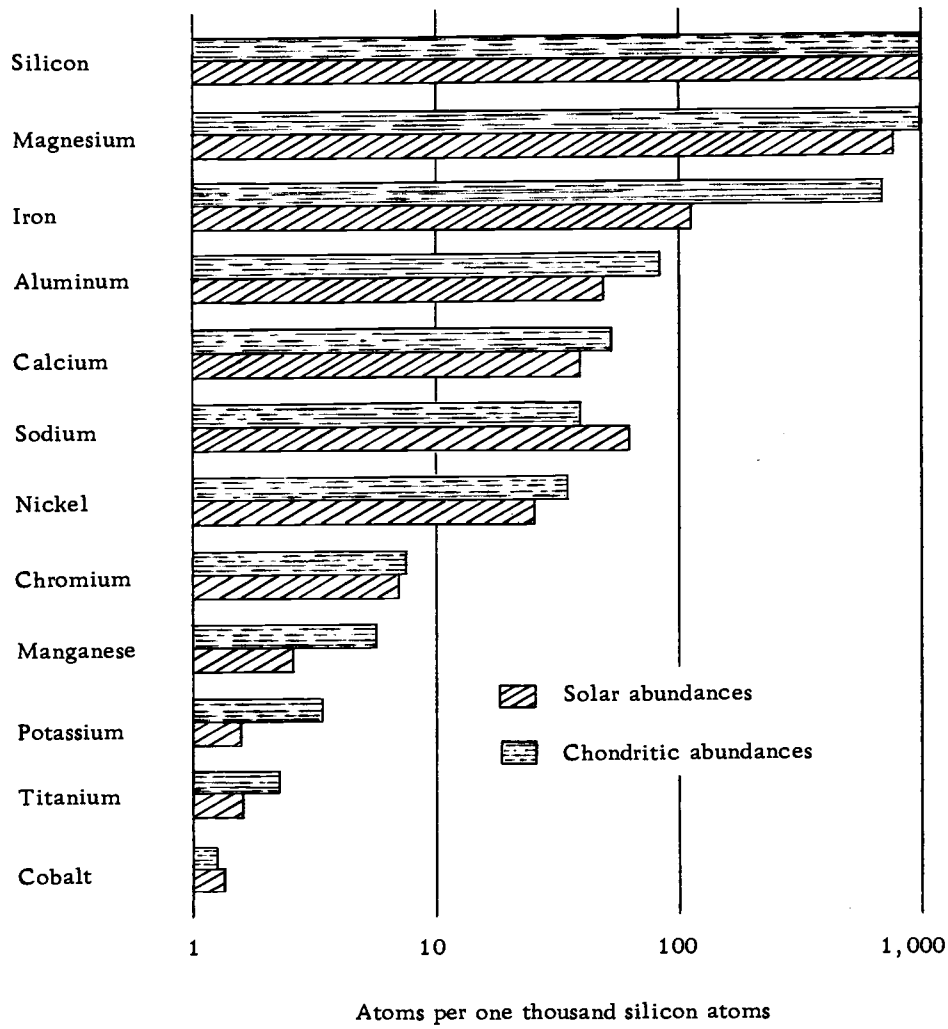

Figure 7. Chondrites and sun, Wood (38).

From the comparisons of these charts it is seen that the chondritic meteorites more closely resemble the solar atmosphere than

terrestrial rock to which we have access. The general homogeneity of chondritic matter, its similarity to the sun and its great age are the best reasons for the belief that meteorites are samples of the primitive solar system.

Origin of Chondrites and Chemical Fractionation

The increased amounts of reliable data, via INAA, on meteorites and superior models of the early solar system (7) have made it possible to propose more quantitative models for the origin of chondrites. The most recent work in this field was by Larimer (15) who gives a condensation history of a cooling gas of cosmic composition to yield the observed chemical fractionation patterns in meteorites. In Larimer's theory the primary fractionation process occurred in the solar nebula rather than in the accreted meteoritic parent body via metamorphism or other processes, such as, volatilization or volcanism, etc.

The basic premise is that meteorites have two types of components resulting from cooling of the primordial cosmic gas. One component which resulted from a fast cooling process yielded pure elements and compounds. The other cooling process was slow and accounted for the formation of alloys and other solid solutions.

The solar nebula in the treatment was assumed to be an ideal gas where the partial pressures of species E is p(E), the atomic

fraction is $N(E)$ and the total pressure is P_T.

$$p(E) = N(E)P_T$$

$$N(E) = n(E) / \sum_{L=H_2}^{i=k} n_i$$

Since H_2 was by far the most abundant substance in the solar nebula an adequate approximation of the atomic fraction is:

$$p(E) = 2A(E)/A(H)P_T$$

where $A(E)$ refers to the abundance of the specific species.

Condensation would then occur when the partial pressure of E equals the vapor pressure of substance E. The following table gives the pressures expected in the solar nebula at various distances from the protosun.

Table 6. Solar nebula pressure (5).

Planet	Orbital Radius	Pressure (atm)
Mercury	0.387	$\sim$17
Earth	1.000	0.6
Asteroids	2.8	6.6×10^{-3}

Ordinary chondrites exhibit abundances for certain elements a magnitude or more lower than those observed for carbonaceous

chondrites. These elements are assumed to have been depleted from their original abundance by a cosmochemical fractionation process. It is significant that the strongly depleted elements such as In, Pb, Bi, Tl, Zn, Cd and Hg are found at the bottom of Table 7, which gives calculated condensation temperatures. These condensation temperatures would be strictly valid if compound formation was inhibited. The inhibition in such a complex system could only be achieved by kinetic considerations of reaction and diffusion rates. In a rapidly cooling system, compound and alloy formation would have been severely restricted by incomplete equilibrium.

Compound condensation has the complication of considering the distribution of an element between various gaseous species. Larimer approaches the problem the following way. Considering the reaction

$$X(g) + Y(g) \rightarrow XY(g)$$

$$K = P(XY)/P(X)P(Y)$$

and K is calculated from

$$\Delta G' = -RT \ln K$$

The system is expressible as an equilibrium system when any two of the intensive variables are expressed, such as temperature and pressure. This was done by setting up simultaneous equations expressing conservation of mass and equilibrium. For example,

Table 7. Condensation temperatures of compounds and elements (11).

Compound or element	P_T 6.6 x 10^{-3} atm. T(°K)
$CaTiO_3$	1740
$MgAl_2O_4$	1680
Al_2SiO_5	1650
$CaAl_2Si_2O_8$	1620
Fe	1620
Ca_2SiO_4	1600
$CaSiO_3$	1580
$CaMgSi_2O_6$	1560
$KAlSi_3O_8$	1470
$MgSiO_3$	1470
SiO_2	1450
Ni	1440
Mg_2SiO_4	1420
$NaAlSi_3O_8$	1320
$MnSiO_3$	1240
MnS	1160
Na_2SiO_3	1160
K_2SiO_3	1120
Cu	1090
Ge	970
Au	920
Ga	880
Zn_2SiO_4	820
Sn	806
Ag	788
ZnS	730
FeS	680
Pb	570
CdS	570
$PbCl_2$	535
Bi	530
Tl	475
Fe_3O_4	400
In	360
H_2O	210
Hg	181

Larimer gives the following mass balance:

$$n(Si) = n(SiO) + n(SiS) + n(SiH_4) + n(SiO_2) + n(Si_2) + n(Si)$$

Considering the two reactions:

$$A) \quad Xg + Yg \rightarrow XYg \quad \Delta G_1^0$$

$$B) \quad Xg + Yg \rightarrow XY_s \quad \Delta G_2^0$$

The vapor pressure was found by the following equation since the activity of the solid is unity.

$$\log P'_{XY} = (\Delta G_2^0 - \Delta G_1^0)/2.303\,RT$$

The condensation temperature was the temperature at which the pressure of XY (Equation A) equals the vapor pressure of XY (Equation B).

From a series of such calculations outlined above Larimer established Table 7.

Additional arguments for solid solutions of the siderophile elements at higher temperatures involves the use of Henery's Law and the assumption that the solutions are ideal.

$$P'(E) = Np^\circ(E)$$

$$P' = [\alpha A(E)/M]\,P^\circ(E)$$

α is the fraction of the trace element of cosmic abundance A(E) which dissolves in a major phase of the cosmic abundance M. P° is the vapor pressure of the pure substance. The gas phase then contains only $(1 - \alpha)$ of the trace element so that the partial pressure becomes:

$$P'(E) = (1 - \alpha)[2A(E)/A(H)]\,P_T$$

When the two pressures are equal the system is in equilibrium. Thus when the cooling rate was slow equilibrium was maintained and diffusion of gases into metal particles (Fe) occurred.

The following diagram gives a condensation history of elements and compounds out of the solar nebula. The shaded region Larimer designates as having the major significance in the condensation sequence. The region between 1350 - 1450° K shows the condensation of Mg and Si as $MgSiO_3$ and Mg_2SiO_4 along with Fe; these are the first major groups to form in the solar nebula. The second shaded area at 1130 - 1100° K is the region where alkali metals would separate out. Since manganese is only a little less volatile than the alkali metals it would follow the same condensation pattern, according to Larimer.

Below 680° K the surface of the metal grains would have been coated with sulfide thus inhibiting further alloy formation and the remaining metals In, Bi, Pb, and Tl competed for the remaining sulfur. These metals are depleted in normal chondrites which Anders (1, 3)

suggested resulted from the mixing of two different materials. This idea was later expanded by Larimer (15) and Larimer and Anders (16) where it was suggested that the depleted fraction resulted from the low temperature fraction via an accretion temperature of 500 - 600 °K which insured incomplete condensation of these elements. It is emphasized, however, that the high and low temperature fractions of different classes of meteorites are not the same (13).

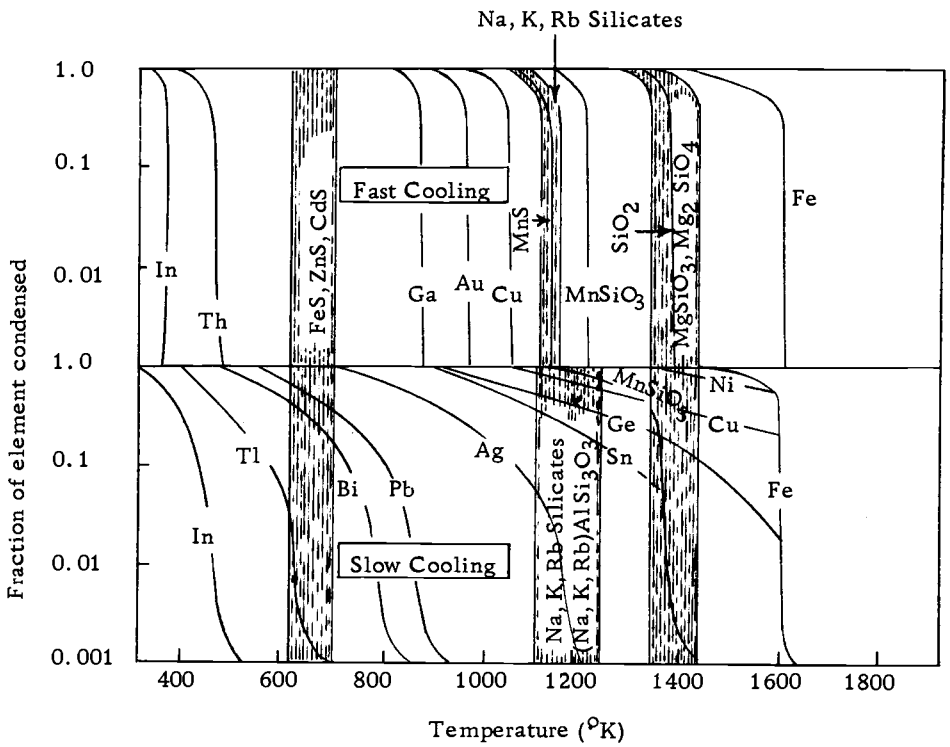

Figure 8. Condensation of material as function of temperature and cooling rate. (Fast cooling--successive layers of pure material condense on grain surface without diffusion. Slow cooling--newly condensed materials diffuse into grain interior forming solid solutions.

Thus it appears that chondrites are a mixture of two fractions: A high temperature portion that lost most of the volatile elements (chondrules and metal grains) and the low temperature portion. The major portion of the cosmochemical fractionation occurred in the solar nebula, perhaps in the asteroid region.

The mode of production of the high and low temperature fractions have been postulated by Wood (32). He believes that shock waves resulting by T Tauri-type eruption compressed and heated ($\geqslant 2000°K$, $\geqslant 10^3$ atm) the nebular gas momentarily. On cooling and and decompression, some of the material passed through a liquid field region of the phase diagram and formed liquid drops. The rest of the material missed the liquid field and condensed directly into micron size dust particles eventually becoming the matrix.

Whipple (37) suggested that turbulent motion of dust and gases in the nebula could result in large electrostatic charges. Intense electrical storms then developed which melted some of the low temperature fraction converting it to the degassed high temperature fraction.

Following condensation the high temperature and low temperature portions then accreted into parent bodies. The mechanism of accretion is not understood but it might have involved gravitational forces and magnetic attraction between particles (40). Larimer and Anders following the idea of small parent bodies postulated the

accretion temperatures on the basis of abundance patterns. The temperatures they arrive at are: Carbonaceous $\leq$ 400° K, Type I enstatite chondrites 400 - 480° K, ordinary and Type II enstatite 530 - 650° K, and unequilibrated ordinary chondrites $\leq$ 530° K. They further point out that these temperatures correspond to distinct regions of the asteroid belt.

Fish, Goles and Anders (9) believe that the parent bodies were asteroidal in size being less than 250 km in radius. They assume that the parent bodies accreted shortly after the nucleosynthesis process so that they were heated by substantial amounts of Al^{26} and Fe^{60} which were incorporated into the parent body. The temperature reached must have been sufficient to melt the core of a small planet and cool in about 10^8 years, a time limit set by Xe^{129} dating.

Ringwood (27) believed that the primary material accreted into bodies of lunar dimensions or larger. Urey (34) proposed that the primary objects of his theory were also this large. These assumptions were based on the formation of meteoritic diamond, cohenite and the Widmanstätten structure in the irons all which needed high pressures to form. Serious objections to lunar sized bodies were summarized by Wood (40).

1. The igneous character of iron and achondrites indicate the core was about 1500° C and a lunar body could not have cooled in the time limit required.

2. Most experts place the meteorites' origin in the Asteroid belt but the total mass is less than 0.03 of the moon. Since mass loss from the Asteroid region is low it would have been difficult to produce a body of lunar size.

3. Large planets are very difficult to break up requiring $\sim$2500 joules/gram.

4. Meteoritic diamond may be formed by shock and certain other high pressure minerals not producable in shock are absent.

5. The Asteroids appear to be primary accretions.

It is evident that the heating of the bodies was intense enough to cause the interior to melt resulting in phase fractionation. The iron and pure metallic phases moved to the center and became the precursor of the irons. On top of the iron core a silicate mantle was present which became the precursor of the achondrites. The exterior portion of the planetesimals underwent metamorphic processes changing the composition and structure to varying degrees depending on the distance from the molten core.

The planetesimals then underwent collisional breakups which resulted in the loss of certain gases. The fragments are continually being perturbed by Mars and Jupiter into earth-collision orbits.

The metamorphic process is evident in the structure of the chondrites.

1. The chondrule structure in some meteorites is very evident

occurring embedded in a dark matrix. In other chondrites they are extremely difficult to distinguish from the matrix since the entire chondrite is very uniform. There is continuous variation between the two extremes. Petrographers have, therefore, concluded that all chondrites had very sharp chondrules but via metamorphism the structure was altered with the original structure being replaced by coarser crystals.

2. The metallic iron phases in chondrites are also characteristic of moderate metamorphic temperatures since a substantial period of heating was necessary to separate the coarser crystals kamacite and taenite from the original high temperature alloy.

3. If as Wood and Cameron (40) suggest the matrix was magnetic with no metallic iron then the Fe^{++} levels in chondrites could have been homogenized by motion of Fe^{++} over short ranges in the solid state.

There is one other important aspect of chemical fractionation occurring in the finds. The weathering processes are known to deplete certain minerals from the meteorite and the degree to which this occurs has not been adequately studied. It is evident, however, that this must be kept in mind when inferring original conditions for meteorite formation from finds.

Instrumental Neutron Activation Analysis

Background

Activation analysis differs from other methods of chemical analysis in that it is based upon the nuclear properties of the elements rather than their chemical properties. It is essentially independent of the chemical matrix in which the nucleus is lodged. Activation analysis also has the advantage of being able to distinguish between isotopes of the same element which is very important in geochemical and cosmochemical studies. The primary virtue of the method lies in its extreme sensitivity and precision. INAA is nondestructive allowing a sample to be reanalyzed many times and still remain intact.

Activation essentially involves the exposure of a target or specimen to a flux of photons or particles with sufficient energy to react with the target nucleus. The activated nucleus is unstable and subsequently decays; the radiation of the decay is detected giving information as to the type and number of nuclei present.

Neutron activation analysis with thermal neutrons is more widely used than any other type of activation. This is a result of several factors: First, there is no coulomb barrier so the neutrons may react with all nuclei. Second, most of the nuclei have large cross sections in the thermal regions. Third, modern reactor

technology has made large thermal-neutron fluxes readily available.

Typical examples of thermal neutron reactions with nuclei are expressed in the two following examples.

$$Na^{23}(n, \gamma)Na^{24}$$

$$Mn^{55}(n, \gamma)Mn^{56}$$

Theory

When an isotope is exposed to a thermal neutron flux and typical reactions as those expressed above proceed the rate of accumulation of the product isotope is equal to its rate of production minus its rate of decay.

$$\frac{dN}{dt} = P - \lambda N$$

dN/dt is the rate of accumulation

P is the rate of production

λ is the decay constant of the product isotope
$= 0.693/t_{1/2}$ (half-life)

N is the number of product nuclei formed.

This equation integrates to

$$\int \frac{dN}{P - \lambda N} = \int dt + C$$

$$-\frac{1}{\lambda}\ln(P - N\lambda) = t_P + \ln C$$

and imposing the condition that $N = 0$ at $t_P = 0$

$$\ln C = -\frac{1}{\lambda}\ln P$$

Therefore,

$$\ln\frac{P - N\lambda}{P} = -\lambda t_P$$

$$\frac{P - N\lambda}{P} = e^{-\lambda t_P}$$

$$N\lambda = P(1 - e^{-\lambda t_P})$$

Since activity, $A = \lambda N$,

$$A = P(1 - e^{-\lambda t_P})$$

The product isotope will continue to decay even after the production of that isotope has ceased, therefore, the activity at some time, t, after the end of bombardment is expressible as:

$$A = P(1 - e^{-\lambda t_P})e^{-\lambda t}$$

The rate of production is expressible as:

$$P = \Phi\sigma N_o$$

where Φ is the thermal-neutron flux; σ is the cross section of the

element; and, N_o is the number of atoms of the element being considered. When a given element has more than one stable isotope it is necessary to use the above parameters in regard to the i^{th} isotope only.

The cross section σ is the probability of a neutron interacting with a given nucleus. The flux is measured in neutrons/cm^2/sec.

Substituting for P

$$A = \Phi \sigma N_o (1 - e^{-\lambda t_P}) e^{-\lambda t}$$

$$N_o = \frac{A e^{\lambda t}}{\Phi \sigma (1 - e^{-\lambda t_P})}$$

The weight of the species being determined is the easily determined by

$$W_u = \frac{A e^{\lambda t} M}{\Phi \sigma (1 - e^{-\lambda t_P}) 6.02 \times 10^{23}}$$

where M is the mole weight.

More often the abundance of the unknown is determined by comparison of the specific activity of a certain γ-ray energy to the specific activity of a known sample. In this type of comparison the following formula is used:

$$W_u = \frac{A_u}{A_s} W_s e^{\lambda t}$$

where the subscripts s and u refer to the standard and unknown respectively, and t is the length of time between counting the standard and the unknown. The comparative method is most often applied for a variety of reasons, the most common being that the flux variation, changes in reactor neutron spectrum and difficulties in accurate measurements of irradiation time cancel out.

Sources of Error

There are three major sources of error associated with neutron activation analysis:

1. Flux inhomogenuities
2. Self-shielding
3. Interfering nuclear reactions.

The problem of flux inhomogenuities for most problems are not severe when simple precautions are taken. Such precautions include using a rotating rack which is adequate unless a very high degree of accuracy is required. Further reference to this problem will be made in the Experimental section.

Self-shielding may be a significant factor in thermal neutron activation when an element with an appreciable cross section is present in sufficient quantities to cause a flux gradient in the sample. At times this problem may be avoided by merely crushing the sample while more complicated corrections are needed at other times.

Interfering nuclear reactions may be classified as two types:

1. Those producing the same radioactive species from a different element by reactions such as (n, p) or (γ, p).

2. Isotopes of other elements may have gamma rays with the same energy as the isotope under consideration. These problems are generally accounted for by considering the exact circumstances and finding a method of subtracting out the interference. A convenient and often used method of correcting for γ interferences involves the relative decay rates of the desired and interfering species. The sample is first counted to obtain information about the short lived isotopes and recounted after the short lived interfering activities have decayed to obtain information on the longer lived isotopes.

In some cosmochemical and geochemical systems the isotopic ratios of elements may differ from what is normally expected and such anomolies must be taken into consideration when establishing the total abundance of an element.

Errors are also associated with the statistical nature of radioactivity. The following is a short discussion of this important feature in activation analysis.

Statistics

The decay of nuclei and the subsequent detection of the gamma radiation is essentially a statistical problem. The decay of a group

of nuclei follows a binomial distribution which is either approximated as a Poisson or Gaussian distribution. The binomial distribution is applied to radioactivity by considering the probability, W(m), of obtaining m disintegrations in a time t from N_o original radioactive atoms.

$$W(m) = \frac{N_o!}{(N_o - m)!\, m!} p^m (1 - p)^{N_o - m}$$

Since

$$\frac{N}{N_o} = e^{-\lambda t}$$

and

$$p = 1 - e^{-\lambda t}$$

$$W(m) = \frac{N_o!}{(N_o - m)!\, m!} (1 - e^{-\lambda t})^m (e^{-\lambda t})^{N_o - m}$$

where p is the probability of decay for a single nucleus and (1 - p) is the probability that the species does not decay. From these basic equations it can be shown (10) that the standard deviation is:

$$\sigma = \sqrt{M}$$

where M is the average number of nuclei which have decayed.

When the proper approximations are made $\lambda t << 1$, $N_o >> 1$, $m << N_o$ and $|M - m| << M$ the Gaussian distribution may be obtained.

$$W(m) = \frac{1}{2\pi m} e^{-(M - m)^2/M}$$

The knowledge of the distribution law allows a quantitative measure of the expected deviation from the mean value to be made. If the error $\epsilon = |M - m|$ and assuming a continuous distribution the normal distribution is represented as:

$$W(\epsilon) = \frac{2}{2\pi M} e^{-\epsilon^2/2m} \, d\epsilon$$

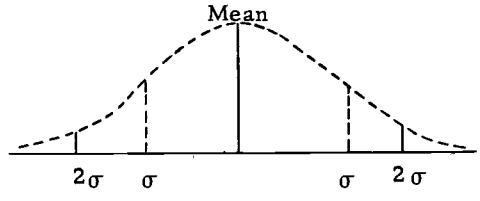

Figure 9. Normal distribution.

Approximately 2/3 of the observed measurements lie within 1σ and 95% lie within 2σ.

When the number of counts in a photopeak are added, subtracted, multiplied or divided the errors or deviations associated with these measurements must be propagated, i. e., carried along. The following propagation formulae are from (10):

$$f = X + Y \qquad e_f = (e_X^2 + e_Y^2)^{1/2}$$

$$f = X - Y \qquad e_f = (e_X^2 + e_Y^2)^{1/2}$$

$$f = XY \qquad e_f = XY\left[\left(\frac{e_X}{X}\right)^2 + \left(\frac{e_Y}{Y}\right)^2\right]^{1/2}$$

$$f = \frac{X}{Y} \qquad e_f = \frac{X}{Y}\left[\left(\frac{e_X}{X}\right)^2 + \left(\frac{e_Y}{Y}\right)^2\right]^{1/2}$$

where e refers to the error associated with a measurement or calculation, in this case, the standard deviation, σ.

Detection

For neutron activation analysis to be considered nondestructive the activity of the sample must be measured without sample destruction. The following portion deals briefly with the radiation detection and analysis systems and corrections for spectrum distortions.

When a gamma ray interacts with matter it may do so by three processes which are functions of $E\gamma$ and the Z of the absorber. The three processes are:

1. Photoelectric effect (low energy interaction)
2. Compton effect (intermediate energy interaction)
3. Pair production (high energy interaction, $E > 1.02$ Mev)

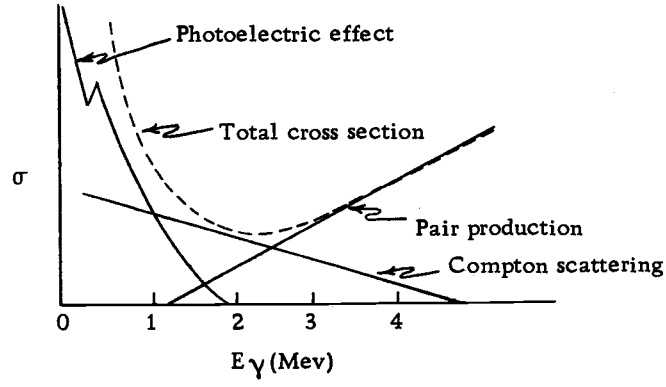

Figure 10. Cross section for gamma ray interaction.

In a scintillator type detector the energy of the γ-ray is deposited in the crystal by producing highly ionizing electrons which then excite the surrounding atoms or molecules. The excited molecule or atom may emit a quantum of light which is detected. The life-time of the excited state is approximately 10^{-8} seconds and decays exponentially. The size of the light pulse is proportional to the energy deposited in the crystal, i. e., the energy of the incident gamma ray. The light then strikes a photocathode and is converted to an electrical pulse whose size is also proportional to $E\gamma$. The pulses are then amplified and sorted according to energy.

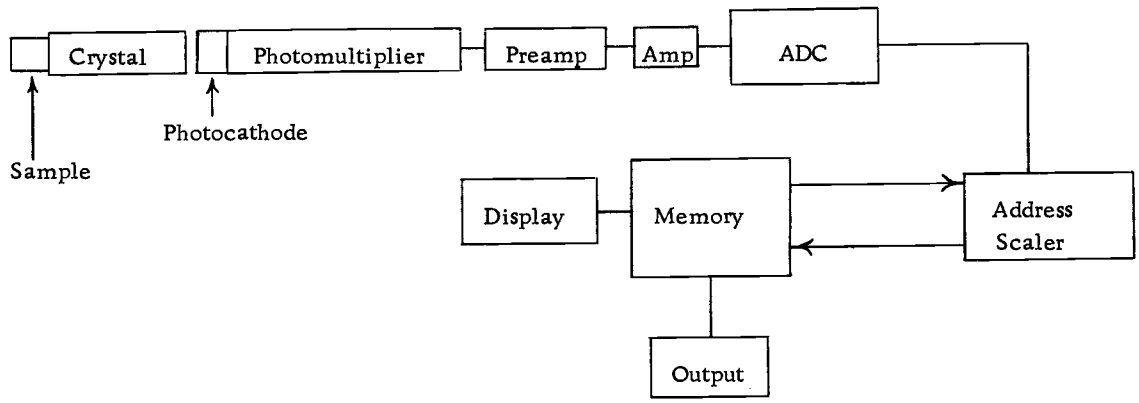

Figure 11. Nuclear detection system.

A pulse height selector serves to sort the sizes of the incoming pulses, thus in effect sorts them into energy ranges. The analog to digital converter (ADC) takes the pulse and converts it into a train of small electrical pulses proportional to the height of the original pulse. The address scaler "counts" the number of little pulses and directs a signal to the appropriate memory position. The memory consists of ferrite memory cores. The display and readout are nondestructive to the memory. In many cases an integrator is present in the system to sum the total pulses in any series of channels in the memory.

When a gamma of intermediate energy interacts with a substance Compton electrons are produced with an energy varying continuously up to a maximum. The maximum energy is

$$E_e = \frac{E}{1 + mc^2/2E}$$

which corresponds to a scatter of 180°. This distribution of electron energies gives rise to what is called a Compton continuum and a Compton edge. It is necessary to eliminate the Compton effects to prevent high energy gamma rays from covering the photopeak of the lower energy gamma rays.

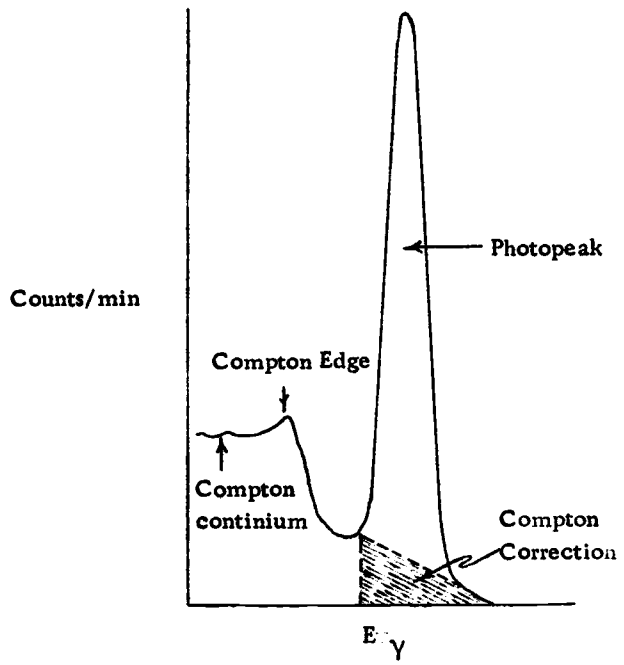

Figure 12. Photopeak showing result of Compton effect.

The most adequate method of eliminating the Compton is determined by the following formula.

$$C = \left[\frac{R + L}{2}\right] n$$

A is the total area of the photopeak

C is the Compton correction

R is the average of two or more channels on the high energy side of the peak.

L is the average of two or more channels on the low energy side of the peak.

n is the number of channels in the photopeak

The net counts in the photopeak is N

$$N = A - C$$

EXPERIMENTAL

Samples

A group of chondritic meteorites for this study was obtained from the Collections of the Center for Meteorite Studies, Arizona State University by the courtesy of Dr. C. B. Moore and Mr. C. F. Lewis. These meteorites were sampled in the following manner.

A given meteorite was placed on a clean sheet of brown wrapping paper and was dusted by use of an air hose to remove accumulated dust and foreign particles which adhered to the meteorite. The importance of this step is easily seen by considering the data given by Bowen and Gibbons (2). The rate of dust accumulation in Cincinnati, Ohio, was determine to be 2.2×10^{-9} g/cm^2/sec and the average amount of manganese in the dust is approximately 3.5×10^{-4} mg Mn/mg of dust. Thus if 10 mg of dust were deposited in approximately ten years this would add 350 ppm of manganese to the determinations.

Each meteorite was sampled in five distinct areas; the distances and relative positions of the individual specimens were recorded. After a single specimen was taken at a position, the hard steel chisel used for sampling was washed with acetone, wiped dry with a Kimwipe and rewashed in acetone to prevent cross contamination of the specimens and to avoid the introduction of organic matter.

Each specimen of the meteorite was separately placed into a two dram polyvial previously washed with acetone. Each specimen weighed approximately one gram. During the entire sampling procedure plastic gloves were worn to prevent contamination of the sample by minerals present on the hands. The plastic gloves were changed after each meteorite had been sampled.

One hundred and twenty-six specimens were studied and were obtained from 23 individual meteoritic stones. These may be classified as follows:

Table 8. Falls and finds analyzed.

	No. of Meteorites	No. of Specimens
Falls	8	51
Finds	10	75

These meteorites may be further classified as:

Table 9. Classes of meteorites analyzed.

	Falls	Finds
Olivine bronzite	2	7
Olivine hypersthene	4	3
Enstatite	0	1

In many cases multiple large fragments of a single large meteorite were samples. In order to obtain a broader perspective

of the homogeneity of these meteorites several such fragments were sampled. Those meteorites in which more than one fragment was sampled are listed below.

Table 10. Meteorites with multiple large fragments.

Meteorites	Fragments Sampled	Total Specimen
Potter	2	14
Plainview	4	20
Holbrook	3	13

Table 11. includes a list of the meteorites sampled and the ASU Catalog number.

All the meteorites in this study fell in the Western United States or Canada.

After the samples had been collected they were carefully crushed in a steel mortar and approximately one gram of the specimen was carefully weighed and placed in a two dram polyvial which had been freshly washed with acetone. The polyvial was labeled to indicate the meteorite, the specimen location and specimen weight. Special care was taken to insure a uniform height of the specimens in the polyvial, so that the vertical flux gradient in the reactor would not be a significant factor. After each specimen was crushed the steel mortar and pestle was washed with acetone and carefully wiped with a Kimwipe to remove specimen particles adhering to the metal.

Table 11. List of meteorites analyzed.

Meteorite	Catalog Number	Weight of Fragment	Date	Type	Specimens
Acme	516.1x	4,1659.7	1947	Cb	5
Atlanta	427.1x	1,480.8	1938	Ce	6
Beardsley	134ax	4,401.8	10/15/29	Cb	6
Bruderheim	705	3,880	3/30/09	Ch	5
Channing	317.1x	2,538.7g	1936	Cb	4
Covert	22Ax	1,136.	1929	Cb	5
Harrisonville	176.24	16,879	1941	Ch	5
Haskel	527.1x	16,896.9	1909	Ch	5
Holbrook	57.75	3,572	7/19/12	Ch	5
Holbrook	H52	3,365	7/19/12	Ch	3
Holbrook	57 g	2,491	7/19/12	Ch	5
Ladder Creek	505hx	5,385	1937	Cb	5
Leedey	489.1	3,502	11/19/12	Ch	5
Maimi	399.1x	29,024.	1937	Cb	5
New Concord	202b	2,301	5/11/60	Ch	5
Plainview	92F	8,833.	1937	Cb	5
Plainview	92gg	5,209.	1937	Cb	5
Plainview	92.995	4,983.	1937	Cb	5
Plainview	92EE	4,983.	1937	Cb	5
Potter	476.67	23,556.	1941	Ch	8
Potter	476.19	15,061.	1941	Ch	5
Richardton	100H	5,775	6/30/18	Cb	5
Texline	415.1x	7,455.7	1937	Cb	5

Key:

Ce enstatite
Cb olivine bronzite
Ch hypersthene
Exact date indicates a fall
Year indicates a find

Then the mortar and pestle were washed again to remove all lint from the Kimwipe. Plastic gloves were worn throughout the entire procedure.

The technique of neutron activation analysis is especially suited for determining gross concentrations of elements in a sample irrespective of its state of chemical combination. The sample was irradiated in a thermal-neutron flux with suitable standards, and then by using the comparative method the amount of element present was determined. The method was non-destructuve since no radiochemical separations were required.

Irradiation

In preparation for irradiation in the Oregon State TRIGA Reactor (OSTR) the specimens were carefully checked to insure that they were approximately of the same height. This step was extremely important in order to obtain precise results since there is an approximate 3% flux gradient per cm rise above the bottom of the TRIGA Tube (33).

In the TRIGA Reactor there is also a radial neutron flux gradient which decreases as the distance from the core increases. Therefore, it was necessary to insure that the polyvials inside the TRIGA Tube were securely centered. This was accomplished simply by wrapping a Kimwipe around the outside of the polyvial to fill up

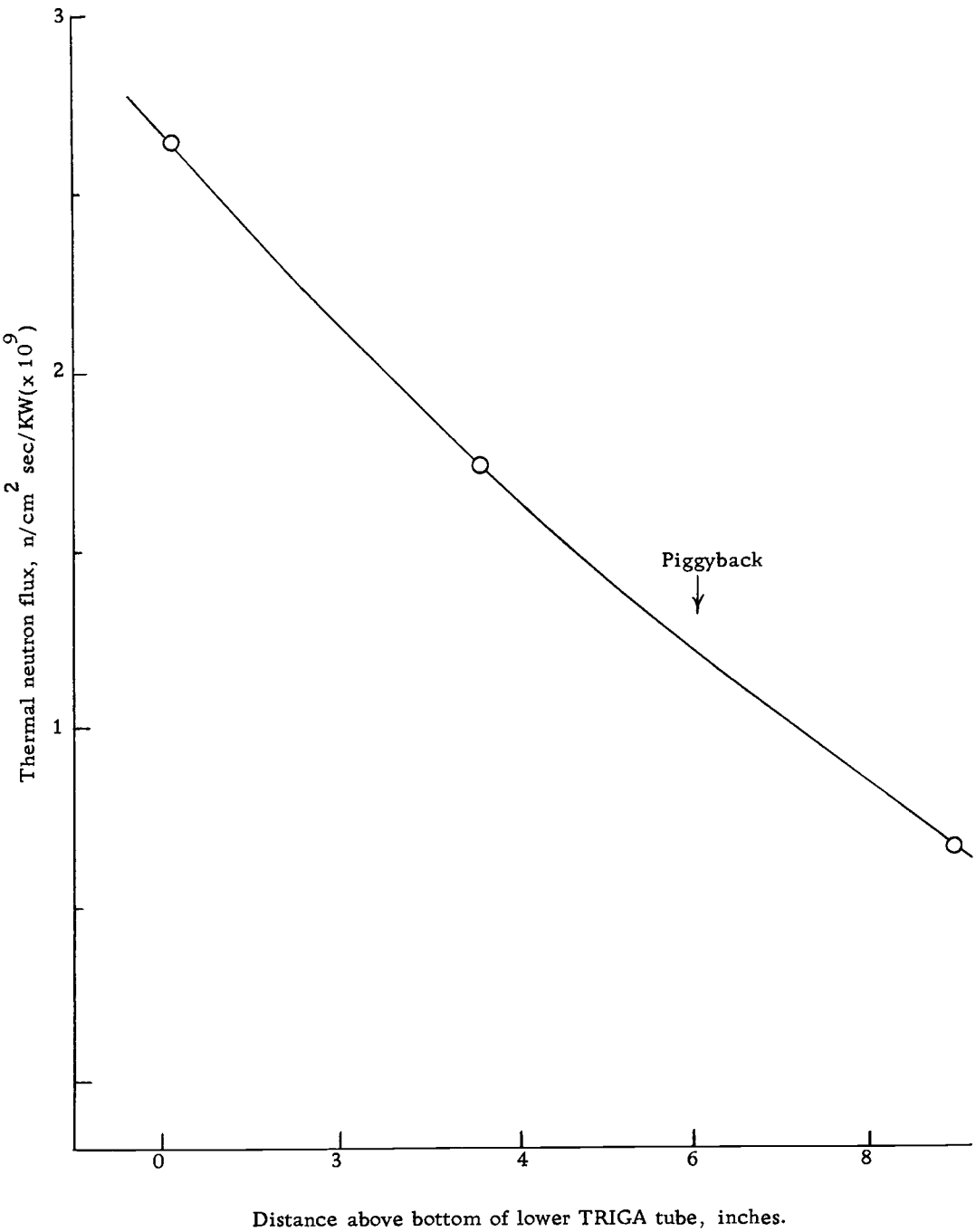

Figure 13. Thermal neutron flux, rotating specimen rack (34).

the excess space in the TRIGA Tube.

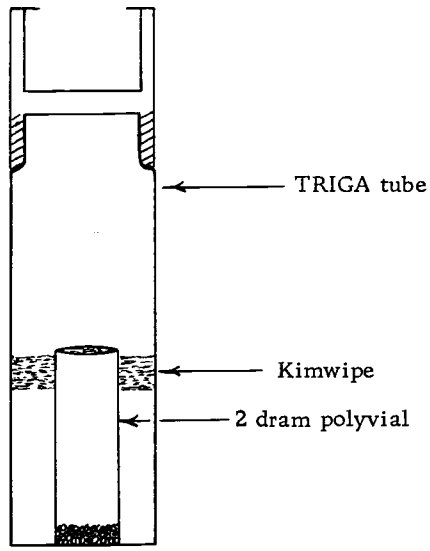

Figure 14. Diagram of loaded TRIGA Tube.

The standards were prepared by using 1.00 ml of 1.01 mg/ml Mn^{++} standard sealed in a two dram polyvial and mounted in the TRIGA Tube in the same manner as the specimens. The sodium standard consisted of 1.00 ml of 5.13 mg/ml Na^{+} solution. The standards were always made in duplicates for the irradiation.

Since the flux in the reactor is very inhomogeneous the specimens and standards were placed in the rotating rack which revolves at approximately 1 rpm. The rotation of the samples insured that they all received a uniform flux. The standards were placed in positions one and two and again in the middle positions. The optimum

irradiation condition was found to be 5 kw for ten minutes.

There is some question as to the degree of homogeneity of the flux even when the samples are placed in the rotating rack. This arises from the nature of the reactor itself.

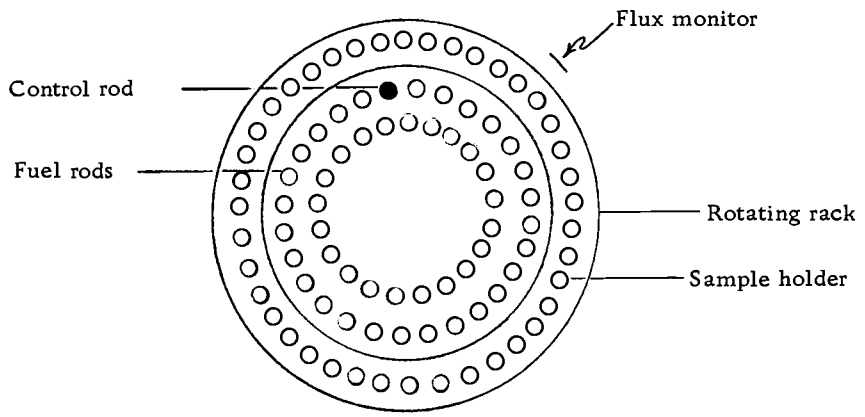

Figure 15. Diagram of rotating rack.

The flux in the reactor is monitored continually and as the specimen passes in front of the monitor it causes an apparent decrease in the flux, so the boron carbide control rod (darkened) rises thereby increasing the reactor power and the neutron flux; when the rod is lowered, the reactor power reaches the proper level again. But in reality the flux has been the same and the monitor saw only an apparent change. Thus, it is possible for the rod to be in phase with a given subgroup of specimens causing them to be exposed to a larger total flux.

This error has been assumed to be no more than a few tenths of a percent but in further highly accurate work this problem should be fully investigated by irradiating a series of standards and comparing their specific activity. If such an effect is apparent there are several possibilities of correcting this problem. A possibility of correcting such an effect lies in the filling of every other position so that in every other position the control monitor would see the full flux. Another possibility for correcting this situation may be simply to turn off the automatic reactor operation mode so the reactor would not compensate for the apparent decrease in flux. If none of these methods adequately corrected the situation then for the most precise work a standard could be irradiated for every specimen.

Another important aspect of the irradiation procedure involves the consideration of delayed neutrons in the reactor after shutdown. The reactor's flux decays by 1/e about every 80 seconds (10) and if the rotating rack is stopped too soon after the irradiation the flux inhomogeneities will cause a significant effect in the sample activity. Also, if the samples are removed too rapidly after shutdown the last sample removed will receive a significantly greater flux than the first sample removed.

Aqueous solutions readily adhere to crevices and indentations of the polyethylene surfaces, (such as the lip and cap of the vial), therefore, it was imperative to exercise extreme caution in the

lowering of the liquid standards into the rack and their subsequent removal after irradiation. If two drops were splashed to the top of a two dram vial and irradiated in that position and in the removal they mixed with the bulk solution again a decrease in solution activity of about 2% would result. This results from the fact that the polyvial is 5.7 cm high and two drops are 10% of the solution volume which was exposed to approximately 20% less flux than the main solution bulk. The above example assumes a 1 ml volume.

To minimize this problem with the standards the polyvial was cut open near the solution surface with great care being taken to avoid causing drops on the sides of the polyvial to run into the bulk solution. An aliquot was taken from the solution bulk and the exact amount was determined by weighing the aliquot.

An alternate and possibly superior method of avoiding droplet formation involves the use of half-dram polyvials. This has the primary advantage that when almost full any splashing or droplet formation would be only a few millimeters above the surface of the liquid. The specimens could also be placed in similar vials so that no relative geometry changes would be present during irradiations. Yet another alternative would be the use of a mock standard in the solid state consisting of SiO_2 and MnO or Na_2O. This would have the advantage of being closer to the actual matrix and splattering would not occur. It might also be a distinct advantage to use a mixture of

Na and Mn rather than independent standards since two of the manganese gamma rays are in coincidence and form a base on which the 2.75 Mev sodium gamma rests. This would make the actual situation more realistic and help to insure greater accuracy.

Each specimen vial after irradiation was carefully wiped with a damp Kimwipe and then dried so as to remove any activity on the exterior of the vial. It is significant to note that in precision work this step is necessary. Bowen and Gibbons showed that if one square centimeter of polyethylene is touched by human hands it gains approximately 4×10^{-7} grams of sodium but only 2×10^{-11} grams of manganese (2). Although this is small, repeated handling before irradiation could cause significant contributions; in addition, there was always a significant amount of contamination gained from oil, etc. on the TRIGA Tube. After the washing procedure a blank showed no appreciable activity.

The basic reactions involved in the analysis were

$$Na^{23}(n, \gamma)Na^{24} \quad t_{1/2} = 14.97 \text{ hrs}$$

$$Mn^{53}(n, \gamma)Mn^{56} \quad t_{1/2} = 2.58 \text{ hrs}$$

The decay schemes for the two unstable nuclei are shown in Figures 16 and 17.

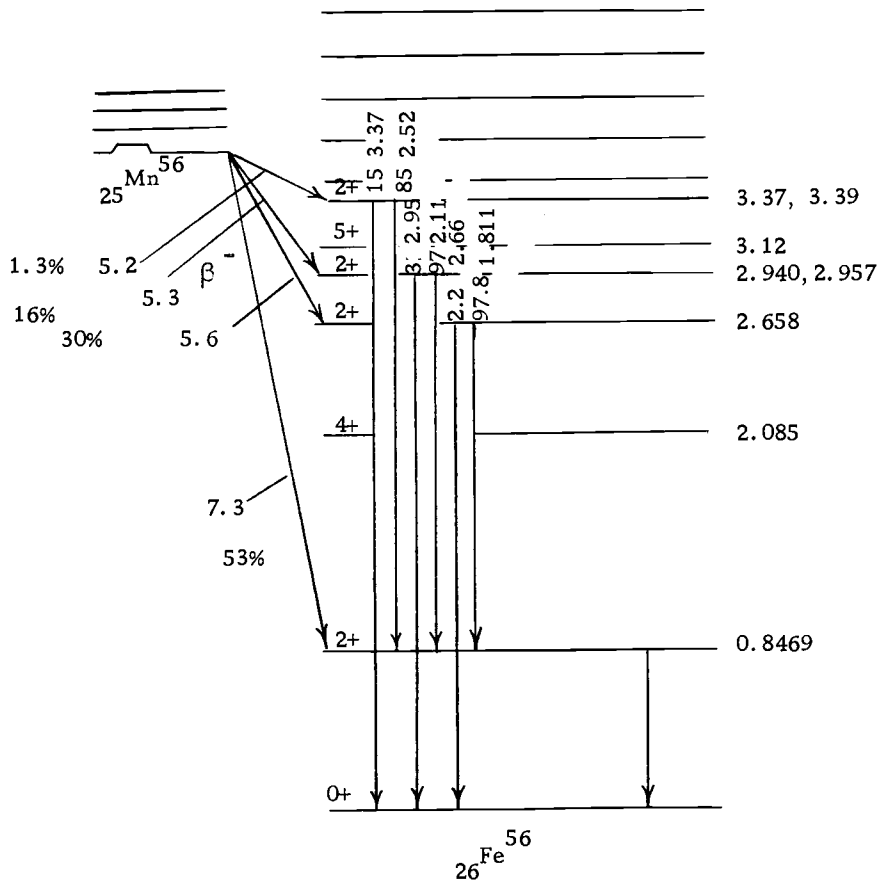

Figure 16. Decay scheme for $_{25}Mn^{56}$ into $_{26}Fe^{56}$ (10).

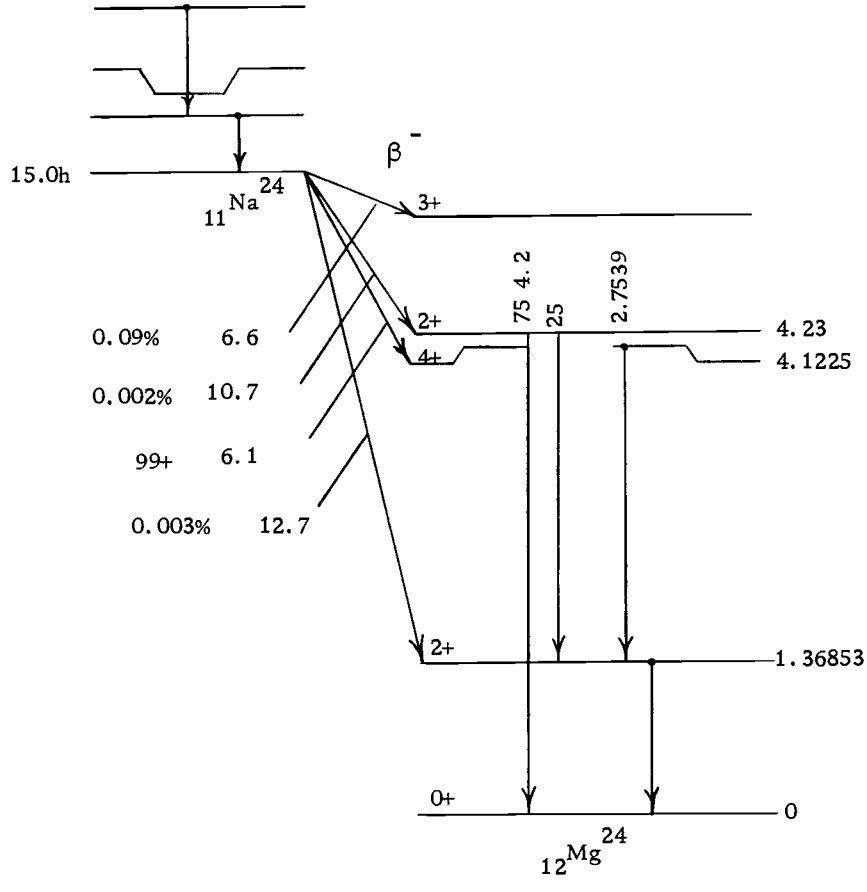

Figure 17. Decay scheme for $_{11}Na^{24}$ into $_{12}Mg^{24}$ (10).

The counting of the samples started approximately three hours after end of bombardment so that the short lived isotope activities would have completely decayed. The actual counting was done on a 3" x 3" NaI(Tl) solid scintillation crystal with a photomultiplier and preamp in conjunction with a 400 channel TMC analyzer. Care was taken so that the percent live time was always greater than 80%, otherwise appreciable channel drift occurred. The counting was usually done in a counting room where the temperature was kept constant since temperature variations also cause appreciable channel drift. In spite of these precautions channel drift did occur and it was necessary to check each tape individually for channel drift.

The two dram polyvials were placed in an elevated geometry 6 cm above the crystal surface for Mn^{56} determination with the geometry being kept identical for each specimen counted. For precision work it was necessary to insure that geometry was reproducible to a very high degree. The following graph shows the effect of sample height on the observed counts, again emphasizing the necessity of uniform sample height. The zero distance is the normal elevated height.

The change in horizontal sample holder position is also important as illustrated by the data in Table 12.

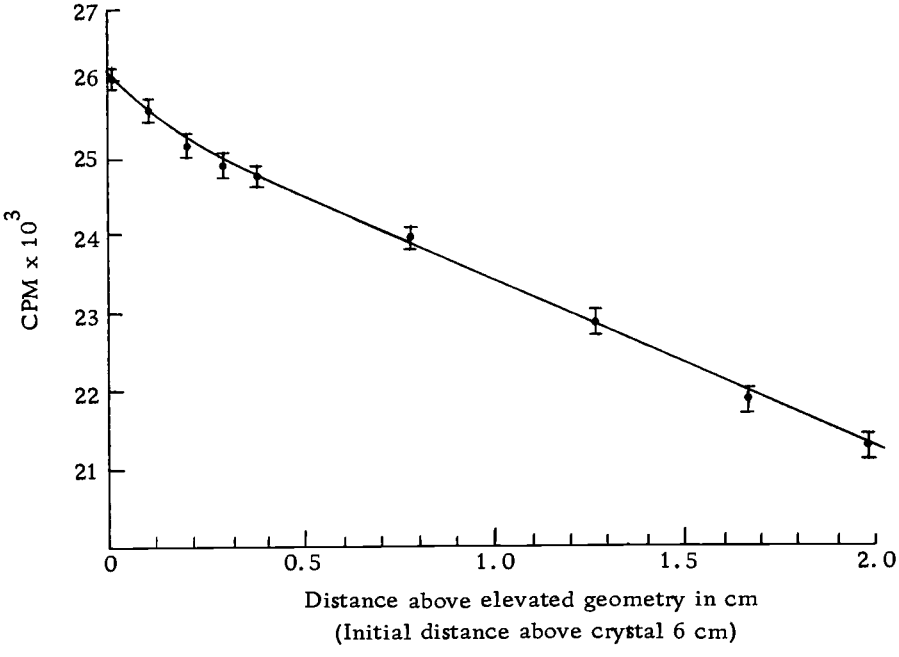

Figure 18. Vertical geometry effects.

Table 12. Horizontal geometry effects.

Position	counts/minute
far right in holder	20840 ± 144
far left in holder	20650 ± 143
change in sample holder	20520 ± 142

Thus it is imperative that great care be taken in placing the sample in the proper geometry and using a tight sample holder to aid in reproducing geometry between specimens. It was found that a small thin plastic tube placed inside of the sample holder of the elevator was tight enough to insure very reproducible geometry.

To reduce natural background the scintillation crystal, photomultiplier and preamp were housed in a lead cave made of St. Joseph's lead which is very low in natural radioactive species.

Each specimen was counted for a length of time adequate to yield about 10,000 counts in the Compton corrected area. In a given irradiation all specimens and standards were counted for the same length of time because it was found that in changing from one minute to four minute counts the observed counts in the photopeak would vary as much as 3% when normalized to a one minute count. This effect apparently resulted from the irreproducibility in the analyzer timing mechanism when changing from one to four minute counts.

The standards were counted several times throughout the counting period in order to establish the decay curves; in any case, where experimental decay curve varied from the literature the experimental half-life, as determined, from the experimental decay curve was used.

The experimental half-life for Mn ranged from about 2.4 to 2.8 hours and for Na from about 14 hours to 17 hours. This deviation resulted presumably from some systematic instrumental error since

a given specimen also decayed with the same half-life as the standards. Even if this effect were not the same for sample and standard the determined homogeneity will still be valid because total counting time for all the specimens of a given meteorite was short compared to the half-life. In the same manner it should be noted that if the total counting time for all the specimens for an irradiation was short compared to the half-life the difference between the experimental and literature value introduced no appreciable error. It was found that if the total counting time was to be less than the half-life the number of specimens were limited to about 20 or 25 per irradiation.

The calculations were performed by comparing the peak areas of the appropriate gamma rays for sample and standards. The peak areas were obtained by summing the total number of counts in each channel under a given peak and subtracting the Compton from the peak. The Compton backgrounds were determined by using the average counts in two or more channels from both the high and low energy sides. The corrected area was then analytically extrapolated to t_o by the experimentally determined $t_{1/2}$.

The sodium abundances were determined approximately 20 hours after the irradiation and all counting was done in the well so the geometry factors were not significant. It was found that the often used technique of using the uncorrected area for the Na^{24} 2.75 Mev gamma ray in the calculations generally gave abundances which were

systematically high ranging from 1% to 5% over the value obtained by using the Compton corrected area.

Several secondary problems had to be considered as to interfering reactions and shielding effects. The 2.75 Mev gamma of the Na^{24} was counted since there are no other gamma rays that would give significant interference at that energy. The major interference of the Mn^{56} results from Sc^{46}, and possibly by very short lived materials. The Mn^{56} was, therefore, counted about three hours after the irradiation so that the short lived species would have decayed away. The long lived Sc^{46} was not a significant problem as can be seen by considering the relative thermal neutron absorption cross sections and abundances (10, 29).

$$\frac{\sigma(Mn^{55})(\text{chondritic abundance})}{\sigma(Sc^{45})(\text{chondritic abundance})} \approx 2000$$

Therefore, in a short irradiation period no significant interference resulted from the activation of Sc^{46}.

The consideration of interfering nuclear reactions is negligible (29, 30). In addition Na^{23} and Mn^{55} are the only stable isotopes of these elements; consequently, it is not necessary to consider anomolies in isotopic distributions. Since the cross sections of Na and Mn are not extremely large and the crystals formed by the minerals are small compared to the sample size, self-shielding is not a significant

factor. Crushing the samples further reduces any such problems.

Sample Calculation

The following is a sample calculation for a typical manganese specimen.

Mn std ($t_{1/2}$ = 2.58 hours)

Corrected area = photopeak area - Compton correction

$$= \text{photopeak area} - \left[\frac{\text{Avg rt channel} + \text{avg left channel}}{2}\right] \text{width}$$

$$= 20000 - \left[\frac{160 + 150 + 210 + 220}{4}\right] 20$$

= 16300

Standard weight = 1.00 mg

Specific activity = 16300 counts/mg Mn

Corrected area specimen = 17, 200

Time counted after standard = 0.70 hours

Activity sample at t_o

$$A^o = Ae^{\lambda t}$$

$$A = 17,200\, e^{(0.693/2.58)0.70}$$

$$= (17,200)(1.21)$$

$$= 20,812 \text{ counts}$$

Specimen weight = 0.5000 grams

$$\text{Counts per mg of specimen} = \frac{20,812}{500 \text{ mg}}$$

$$= 41.6 \text{ count/mg of specimen}$$

$$\text{ppm} = \frac{\text{specific activity specimen}}{\text{specific activity standard}} \times 10^6$$

$$\frac{41.6}{16,300} \times 10^6$$

$$= 2550 \text{ ppm Mn}$$

The sodium abundances were determined in an identical manner using t_o to be the initial time the standard was counted.

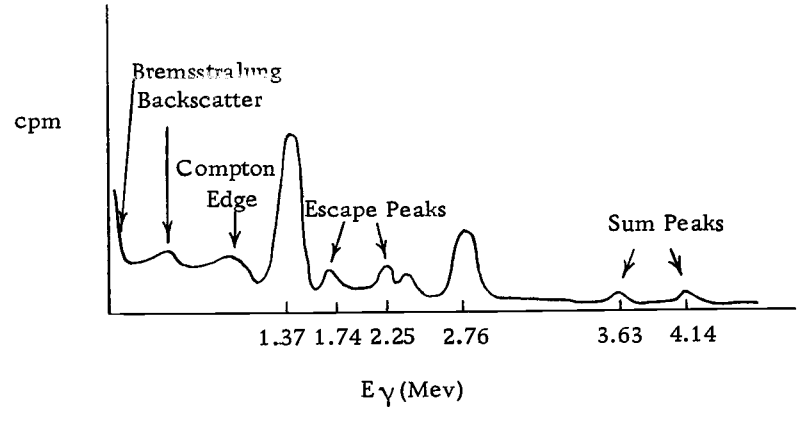

Figure 19. Typical gamma spectrum of Na^{24}.

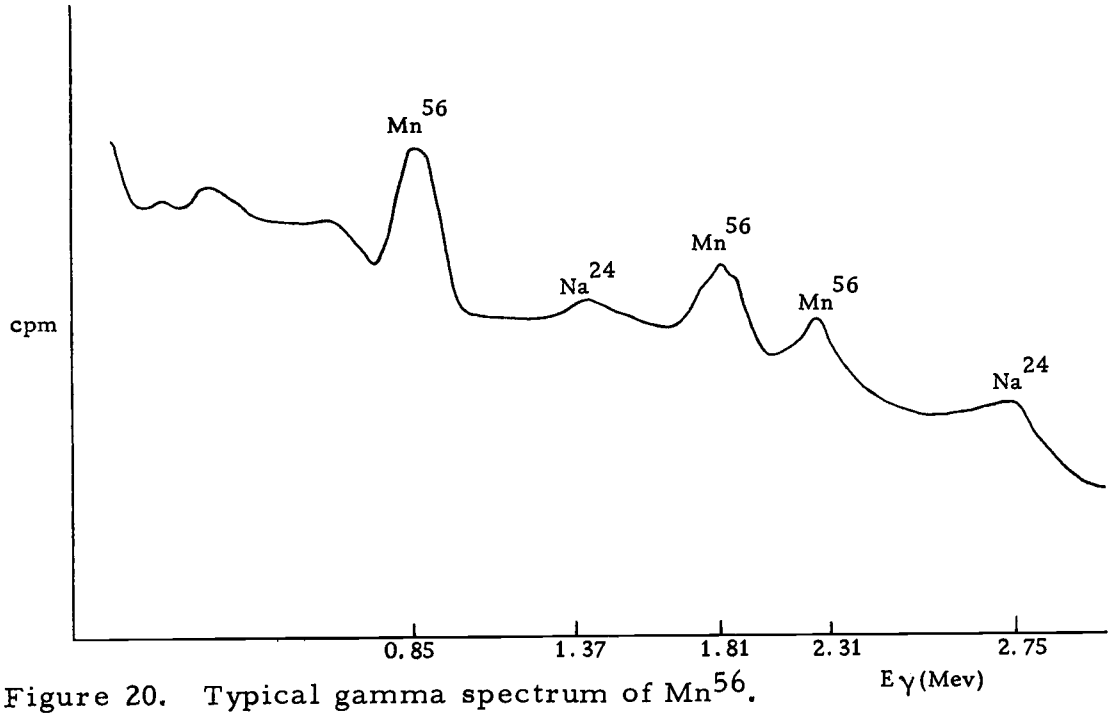

Figure 20. Typical gamma spectrum of Mn^{56}.

Precision and Accuracy

It should be noted at the outset of this portion of the discussion that precision and accuracy are not interchangable terms. Statistical methods give a quantitative measure of precision and not of accuracy. There are many factors which effect the accuracy and the precision of this work. The primary consideration is that of statistics. When the error is propagated for the entire calculation via the formulas given earlier it was found that there must be about 10, 000 counts in the corrected photopeak area in order to insure statistics of about 1%. In addition cognizance of the statistical

nature of radioactive decay must necessarily result in realizing about 1/3 of the measurements are more than one standard deviation from the mean value. Thus when comparing two separated irradiations of the same specimens one would expect at least 1/3 of the values to lie outside of the assigned error limits. Also one might expect that if two values were compared one might have had a deviation of $+\sigma$ for one measurement and $-\sigma$ for the other; thus the difference between the two values would be 2σ.

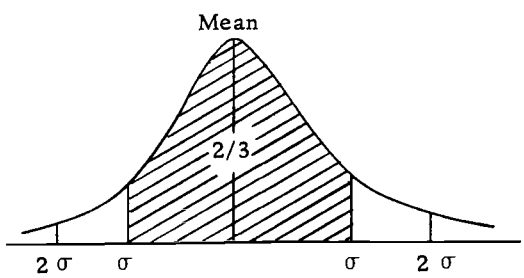

Figure 21. Distribution of radioactive measurements.

It is, therefore, necessary to exercise extreme care in determining which values are truly within 1σ of the mean, and which values should be rejected. This problem becomes significant when a high degree of precision is required. There are two methods which help

to avoid this pitfall:

1. Irradiate the specimens more than once which provides an independent check on the values.

2. Count each specimen several times for a given irradiation.

It was found to be a prudent procedure to reirradiate several previous specimens with each new irradiation. This has a twofold purpose: first, it provided a continual check on internal consistancy. Second, in cases where the specific activity of the two standards showed a discrepancy due to splashed droplets being irradiated and remixed with the bulk solution or any associated problem they allowed the choice of the correct standard.

The total precision of the determination was placed at about 1.5% which allows for flux inhomogenuity, geometry variation, etc.

There are undoubtedly some values which exhibit a deviation greater than one standard deviation from the mean value but these should be very few since many of the samples were repeated and counted numerous times. Also any value which is exceedingly high or low in comparison to the other values obtained for the given meteorite was specifically rechecked, so such anomalies should be regarded as real.

There is no significant reason to assume that the accuracy differs from the precision (30) but even if this were the case, the relative values would remain the same. Consequently,

any conclusions on the homogeneity of these meteorites will be valid irrespective of the absolute values since the relative values will remain consistent among themselves.

DATA

Olivine bronzites

Table 13. Olivine Bronzite Chondrites.

Falls

SET : 1 (Richardton 100H) H5

Specimen	Mn Abundance (PPM)	Na Abundance (PPM)
1	2180 ± 25	6020 ± 90
2	1990 ± 30	5280 ± 80
3	2130 ± 24	5820 ± 87
4	2140 ± 25	5600 ± 84
5	2200 ± 26	5970 ± 90

SET : 2 (Beardsley 134Ax) H5

Specimen	Mn Abundance (PPM)	Na Abundance (PPM)
1	2350 ± 35	5390 ± 81
2	2310 ± 35	5790 ± 87
3	2250 ± 34	5580 ± 84
4	2310 ± 39	5630 ± 84
5	2340 ± 35	5090 ± 76

Table 14. Olivine Bronzite Chondrites.

Finds (A)

SET : 1 (Plainview 92.995) H5

Specimen	Mn Abundance (PPM)	Na Abundance (PPM)
1	2440 ± 36	5340 ± 80
2	2380 ± 36	6090 ± 91
3	2280 ± 34	5650 ± 85
4	2430 ± 24	5650 ± 85
5	2350 ± 35	5620 ± 84

SET : 2 (Plainview 92F) H5

Specimen	Mn Abundance (PPM)	Na Abundance (PPM)
1	2270 ± 36	5450 ± 82
2	2300 ± 34	5640 ± 85
3	2330 ± 23	5560 ± 84
4	2340 ± 35	5630 ± 85
5	2300 ± 34	5710 ± 80

SET : 3 (Plainview 92qq) H5

Specimen	Mn Abundance (PPM)	Na Abundance (PPM)
1	2340 ± 35	5260 ± 79
2	2380 ± 36	5750 ± 86
3	2350 ± 40	5500 ± 83
4	2400 ± 36	5340 ± 80
5	2350 ± 36	5350 ± 80

SET : 4 (Plainview 92EE) H5

Specimen	Mn Abundance (PPM)	Na Abundance (PPM)
1	2240 ± 34	5520 ± 83
2	2220 ± 34	5850 ± 88
3	2260 ± 34	5860 ± 88
4	2240 ± 34	5470 ± 84
5	2310 ± 25	5630 ± 85

SET : 5 (Texline 415.1x) H5

Specimen	Mn Abundance (PPM)	Na Abundance (PPM)
1	2340 ± 40	5880 ± 70
2	2320 ± 38	5870 ± 88
3	2290 ± 37	6340 ± 95
4	2320 ± 38	5960 ± 89
5	2300 ± 37	5900 ± 94

Table 15. Olivine Bronzite Chondrites.

Finds (B)

SET : 1 (Channing 317. 1x) H5

Specimen	Mn Abundance (PPM)	Na Abundance (PPM)
1	2090 ± 31	4860 ± 72
2	1550 ± 23	4400 ± 44
3	2200 ± 33	5000 ± 75
4	2170 ± 33	4970 ± 75

SET : 2 (Covert 22Ax) H5

Specimen	Mn Abundance (PPM)	Na Abundance (PPM)
1	2050 ± 30	2990 ± 45
2	2250 ± 34	5060 ± 130
3	2330 ± 35	3950 ± 59
4	1840 ± 28	2780 ± 42
5	2140 ± 30	3590 ± 54

SET: : 3 (Acme 516. 1x) H5

Specimen	Mn Abundance (PPM)	Na Abundance (PPM)
1	2100 ± 32	4980 ± 75
2	1960 ± 30	4880 ± 73
3	1950 ± 30	4700 ± 71
4	2010 ± 30	4620 ± 70
5	2120 ± 32	5060 ± 76

SET : 4 (Maimi 399. 1x) H5

Specimen	Mn Abundance (PPM)	Na Abundance (PPM)
1	2150 ± 35	4800 ± 72
2	2000 ± 24	4480 ± 67
3	2260 ± 25	5080 ± 76
4	2070 ± 25	5030 ± 76
5	2090 ± 34	5020 ± 75

Olivine Hypersthenes

Table 16. Olivine Hypersthene Chondrites.

Falls

SET : 1 (Leedey 489.14x) L6

Specimen	Mn Abdunance (PPM)	Na Abundance (PPM)
1	2630 ± 30	6590 ± 80
2	2550 ± 38	7610 ± 114
3	2550 ± 38	7610 ± 114
4	2550 ± 38	7050 ± 110
5	2590 ± 39	7750 ± 116

SET : 2 (New Concord 202b) L6

Specimen	Mn Abundance (PPM)	Na Abundance (PPM)
1	2580 ± 39	7520 ± 113
2	2520 ± 38	7370 ± 110
3	2440 ± 26	7160 ± 108
4	2560 ± 38	7400 ± 111
5	2490 ± 37	7030 ± 105

SET : 3 (Holbrook 57G) L6

Specimen	Mn Abundance (PPM)	Na Abundance (PPM)
1	2440 ± 37	8170 ± 123
2	2320 ± 35	8200 ± 123
3	2350 ± 35	8250 ± 124
4	2520 ± 38	8390 ± 126
5	2360 ± 35	7620 ± 115

SET : 4 (Holbrook 57.75) L6

Specimen	Mn Abundance (PPM)	Na Abundance (PPM)
1	2470 ± 37	7640 ± 114
2	2470 ± 37	7620 ± 114
3	2440 ± 37	7650 ± 115
4	2550 ± 33	7550 ± 113
5	2420 ± 36	7650 ± 115

SET : 5 (Holbrook H52) L6

Specimen	Mn Abundance (PPM)	Na Abundance (PPM)
1	2410 ± 36	8020 ± 120
2	2370 ± 36	7730 ± 116
3	2320 ± 30	7790 ± 117

SET : 6 (Bruderheim 705) L6

Specimen	Mn Abundance (PPM)	Na Abundance (PPM)
1	2400 ± 36	6540 ± 98
2	2500 ± 38	6960 ± 105
3	2550 ± 38	6540 ± 98
4	2440 ± 25	6900 ± 105
5	2410 ± 36	6440 ± 97

Table 17. Olivine Hypersthene Chondrites.

Finds

SET : 1 (Ladder Creek 405 hx) L6

Specimen	Mn Abundance (PPM)	Na Abundance (PPM)
1	2440 ± 40	6440 ± 120
2	2350 ± 38	6390 ± 96
3	2490 ± 40	6190 ± 93
4	2430 ± 39	6340 ± 95
5	2350 ± 38	6380 ± 96

SET : 2 (Harrisonville 176.24) L6

Specimen	Mn Abundance (PPM)	Na Abundance (PPM)
1	2500 ± 40	5970 ± 90
2	2330 ± 25	6600 ± 120
3	2370 ± 38	5650 ± 85
4	2490 ± 40	5690 ± 85
5	2580 ± 41	6120 ± 90

SET : 3 (Haskell 527.1x) L6

Specimen	Mn Abundance (PPM)	Na Abundance (PPM)
1	2570 ± 41	6080 ± 91
2	2430 ± 39	6200 ± 93
3	2370 ± 40	5520 ± 83
4	2450 ± 30	6370 ± 97
5	2430 ± 39	6100 ± 91

SET : 4 (Potter 476.19) L6

Specimen	Mn Abundance (PPM)	Na Abundance (PPM)
1	2340 ± 35	5960 ± 90
2	2260 ± 34	5610 ± 85
3	2280 ± 60	5680 ± 85
4	2450 ± 37	5970 ± 90
5	2590 ± 26	5740 ± 85
6	2360 ± 35	6120 ± 92

SET : 5 (Potter 476.67) L6

Specimen	Mn Abundance (PPM)	Na Abundance (PPM)
1	2660 ± 40	6850 ± 103
2	2530 ± 50	5580 ± 84
3	2380 ± 36	6390 ± 96
4	2400 ± 36	6860 ± 103
5	2380 ± 36	6500 ± 98
6	2330 ± 35	5950 ± 89
7	2340 ± 35	6200 ± 93
8	2430 ± 35	5810 ± 88

Enstatites

Table 18. Enstatite Chondrites.

Finds

SET : 1 (Atlanta 427.1x) E5

Specimen	Mn Abundance (PPM)	Na Abundance (PPM)
1	2060 ± 32	4380 ± 66
2	540 ± 32	3940 ± 39
3	1350 ± 25	4220 ± 63
4	1290 ± 20	4770 ± 71
5	850 ± 30	2720 ± 27
6	960 ± 20	4730 ± 71

STATISTICAL CALCULATIONS

Population Means and Fractional Standard Deviations

Olivine Bronzites (H5)

Table 19. Olivine Bronzite Chondrites - Falls.

Mean and Population Standard Deviation

	Manganese			Sodium		
Sets	Mean (PPM)	PSD (PPM)	FSD	Mean (PPM)	PSD (PPM)	FSD
1. Richardton	2130	82	0.038	5740	303	0.052
2. Beardsley	2310	39	0.017	5480	269	0.049
Grand Value	2200	114	0.052	5620	299	0.053

Table 20. Mean and Population Standard Deviation.

(Mean and PSD are weighted by inverse square of standard deviation.)

	Manganese			Sodium		
Sets	Mean (PPM)	PSD (PPM)	FSD	Mean (PPM)	PSD (PPM)	FSD
1. Richardton	2140	83	0.039	5710	304	0.052
2. Beardsley	2310	39	0.017	5470	269	0.049
Grand Value	2200	117	0.053	5590	300	0.054

Table 21. Olivine Bronzite Chondrites - Finds (A)

Mean and Population Standard Deviation

	Manganese			Sodium		
Sets	Mean (PPM)	PSD (PPM)	FSD	Mean (PPM)	PSD (PPM)	FSD
1. Plainview 92.995	2380	65	0.027	5670	269	0.047
2. Plainview 92F	2310	28	0.012	5600	98	0.018
3. Plainview 92qq	2360	25	0.011	5440	194	0.036
4. Plainview 92EE	2250	34	0.015	5670	182	0.032
5. Texline	2310	19	0.008	5990	199	0.033
Grand Value	2320	56	0.024	5670	255	0.045

Table 22. Olivine Bronzite Chondrites - Finds (A)

Mean and Population Standard Deviation
(Mean and PSD are weighted by inverse square of standard deviation.)

	Manganese			Sodium		
Sets	Mean (PPM)	PSD (PPM)	FSD	Mean (PPM)	PSD (PPM)	FSD
1. Plainview 92.995	2380	66	0.027	5650	269	0.048
2. Plainview 92F	2310	28	0.012	5600	98	0.018
3. Plainview 92qq	2360	25	0.011	5400	194	0.036
4. Plainview 92EE	2260	35	0.015	5660	182	0.032
5. Texline	2310	20	0.008	5970	200	0.034
Grand Value	2320	56	0.024	5660	256	0.045

Table 23. Olivine Bronzite Chondrites - Finds (B)

Mean and Population Standard Deviation

	Manganese			Sodium		
Sets	Mean (PPM)	PSD (PPM)	FSD	Mean (PPM)	PSD (PPM)	FSD
1. Channing	2000	305	0.153	4810	278	0.058
2. Covert 22Ax	2120	190	0.090	3670	904	0.246
3. Acme	2030	78	0.038	4850	185	0.038
4. Maimi	2110	98	0.046	4880	249	0.051
Grand Value	2070	172	0.083	4540	706	0.152

Table 24. Mean and Population Standard Deviation.

(Mean and PSD are weighted by inverse square of standard deviation.)

	Manganese			Sodium		
Sets	Mean (PPM)	PSD (PPM)	FSD	Mean (PPM)	PSD (PPM)	FSD
1. Channing	1910	322	0.169	4690	316	0.067
2. Covert 22Ax	2100	193	0.092	3270	1010	0.308
3. Acme	2020	78	0.038	4840	186	0.038
4. Maimi	2110	98	0.046	4860	250	0.052
Grand Value	2040	175	0.085	4220	778	0.184

Olivine Hypersthenes (L6)

Table 25. Olivine Hypersthene Chondrites - Falls.

Mean and Population Standard Deviation

	Manganese			Sodium		
Sets	Mean (PPM)	PSD (PPM)	FSD	Mean (PPM)	PSD (PPM)	FSD
1. Leedey	2570	36	0.014	7320	490	0.067
2. New Concord	2520	56	0.022	7300	197	0.027
3. Holbrook 57G	2400	81	0.034	8130	295	0.036
4. Holbrook 57.75	2470	49	0.020	7620	42	0.006
5. Holbrook H52	2370	45	0.019	7850	153	0.020
6. Bruderheim	2460	64	0.026	6680	236	0.035
Grand Value	2470	86	0.035	7460	539	0.072

Table 26. Olivine Hypersthene Condrites - Falls.

Mean and Population Standard Deviation
(Mean and PSD weighted by inverse square of standard deviation.)

	Manganese			Sodium		
Sets	Mean (PPM)	PSD (PPM)	FSD	Mean (PPM)	PSD (PPM)	FSD
1. Leedey	2580	36	0.014	7190	510	0.071
2. New Concord	2500	58	0.023	7290	198	0.027
3. Holbrook 57G	2390	81	0.034	8110	299	0.037
4. Holbrook 57.75	2470	50	0.020	7620	42	0.006
5. Holbrook H52	2360	46	0.019	7840	153	0.020
6. Bruderheim	2450	64	0.026	6660	237	0.036
Grand Value	2470	85	0.034	7360	547	0.074

Table 27. Olivine Hypersthene Chondrites - Finds.

Mean and Population Standard Deviation

	Manganese			Sodium		
Sets	Mean (PPM)	PSD (PPM)	FSD	Mean (PPM)	PSD (PPM)	FSD
1. Ladder Creek	2410	61	0.025	6350	95	0.015
2. Harrisonville	2460	102	0.042	6010	385	0.064
3. Haskell	2450	73	0.030	6050	320	0.053
4. Potter 476.19	2380	122	0.051	5850	199	0.034
5. Potter 476.67	2430	111	0.046	6270	470	0.075
Grand Value	2420	97	0.040	6110	366	0.060

Table 28. Mean and Population Standard Deviation.

(Mean and PSD weighted by the inverse square of the standard deviation.)

	Manganese			Sodium		
Sets	Mean (PPM)	PSD (PPM)	FSD	Mean (PPM)	PSD (PPM)	FSD
1. Ladder Creek	2410	61	0.025	6340	96	0.015
2. Harrisonville	2420	108	0.049	5940	393	0.066
3. Haskell	2450	73	0.030	6020	322	0.053
4. Potter 476.19	2420	129	0.053	5840	199	0.034
5. Potter 476.67	2420	112	0.046	6210	475	0.076
Grand Value	2420	97	0.040	6060	370	0.061

Enstatites (E5)

Table 29. Enstatite Chondrites - Finds.

Mean and Population Standard Deviation

	Manganese			Sodium		
Sets	Mean (PPM)	PSD (PPM)	FSD	Mean (PPM)	PSD (PPM)	FSD
1. Atlanta	1180	526	0.446	4130	757	0.184

Table 30. Mean and Population Standard Deviation.

(Mean and PSD are weighted by inverse square of standard deviation.)

	Manganese			Sodium		
Sets	Mean (PPM)	PSD (PPM)	FSD	Mean (PPM)	PSD (PPM)	FSD
1. Atlanta	1170	526	0.446	3530	997	0.283

Correlation Coefficients

Table 31. Correlation coefficients of Olivine Bronzite - Falls.

Set	Correlation Coefficient	
	Unweighted Mean	Inverse sq. Weighted Mean
1. Richardton	0.93	0.91
2. Beardsley	-0.51	-0.51
Grand Value	-0.13	-0.10

Table 32. Correlation coefficients of Olivine Bronzite - Finds (A).

Set	Correlation Coefficient	
	Unweighted Mean	Inverse.sq. Weighted Mean
1. Potter 476.19	0.17	0.15
2. Potter 476.67	0.18	0.20
3. PLV 92.995	-0.25	-0.25
4. PLV 92F	0.42	0.41
5. PLV 92qq	0.31	0.31
6. PLV 92EE	-0,09	-0.10
7. Acme	0.73	0.73
8. Texline	-0.70	-0.69
9. Maimi	0.64	0.64
Grand Value	0.73	0.73

Table 33. Correlation coefficients of Olivine Bronzite - Finds (B).

Set	Correlation Coefficient	
	Unweighted Mean	Inverse sq. Weighted Mean
1. Channing	1.0	0.98
2. Covert	0.78	0.76
3. Acme	0.73	0.73
4. Maimi	0.64	0.64
Grand Value	0.28	0.28

Table 34. Correlation coefficients of Olivine Hypersthene - Falls.

Set	Correlation Coefficients	
	Unweighted Mean	Inverse sq. Weighted Mean
1. Leedey	-0.59	-0.61
2. New Concord	0.83	0.80
3. Holbrook 57G	0.43	0.44
4. Holbrook 57.75	-0.96	-0.96
5. Holbrook H52	0.71	0.70
6. Bruderheim	0.24	0.25
Grand Value	-0.30	-0.29

Table 35. Correlation coefficients of Olivine Hypersthene - Finds.

Set	Correlation Coefficients	
	Unweighted Mean	Inverse sq. Weighted Mean
1. Ladder Creek	-0.62	-0.61
2. Harrisonville	-0.74	-0.64
3. Haskell	0.45	0.45
4. Potter 476.19	0.17	0.15
5. Potter 476.67	0.18	0.20
Grand Value	-0.22	-0.22

Table 36. Correlation coefficients of Enstatites-Find.

Set	Correlation Coefficients	
	Unweighted Mean	Inverse sq. Weighted Mean
1. Atlanta	0.38	0.38

RESULTS

Statistical Calculations Used in Discussion

The mean values were calculated by (26)

$$m = \frac{X_1 + X_2 + \cdots X_n}{n}$$

$$= \sum_{i}^{n} X_i/n$$

The means weighted by the inverse square of the standard deviation were calculated by the following formula (26)

$$m^W = \frac{\sum_{i=1}^{n} X_i/S_i^2}{\sum_{i=1}^{n} 1/S_i^2}$$

The grand mean was calculated by using

$$\overline{\overline{X}} = \sum_{i=1}^{N} \overline{X}_i/N$$

and the grand weighted mean was calculated using (26)

$$\bar{\bar{X}}^W = \frac{\sum_{i=1}^{N} \bar{X}_i / S_{\bar{X}i}^2}{\sum_{i=1}^{N} 1/S_{\bar{X}_i}^2}$$

The population standard deviations for the mean and grand mean were determined by the following formula (26):

$$S = \left(\frac{\sum_{i=1}^{N} (X_i - m)^2}{n - 1}\right)^{1/2}$$

and the standard deviation of the means weighted by the inverse square of the standard deviations of the individual measurements was calculated by

$$S^w = \left(\frac{\sum 1/S_i^2 (X_i - m^w)^2}{\sum 1/S_i^2}\right)^{1/2}$$

The correlation coefficients may be expressed by (26)

$$r = \frac{\sum w_i (X_i - \bar{X}^w)(Y_i - \bar{Y}^w)}{\sum w_i (X_i - \bar{X}^w)^2 \sum w_i (Y_i - \bar{Y}^w)^2}$$

where the weighting coefficients may be unity or $1/S_i^2$.

Since the unweighted and inverse square weighted abundance values give the best estimate of the homogeneity of the parent bodies they are used in the interpretation of the data. The mass weighted values does not give the best estimate of the homogeneity of the parent body because there is no known correlation between:

1. The mass of the fragment entering the atmosphere and the mass of the fragment sampled.

2. The mass of the fragment entering the atmosphere and the mass of the parent body.

It can be shown (26) that for the best statistical estimate of a mean and its associated standard deviation the individual measurements should be weighted by the inverse square of its standard deviation. Although the weighted and unweighted values are given, only the inverse square weighted values will be considered further since they have both the greatest physical and statistical significance.

In the study of homogeneity it is necessary to determine if two values or sets of values belong to the same population. If the two means belong to the same population they are considered to be consistent. A criteria for the consistency of two means is when the difference between $\overline{X}_1 - \overline{X}_2$ is less than the standard deviation of the difference between the two means (26). That is:

$$\overline{X}_1 = \overline{X}_2$$

If

$$S_{(\overline{X}_1 - \overline{X}_2)} > |\overline{X}_1 - \overline{X}_2|$$

$$\sqrt{S^2_{\overline{X}_1} + S^2_{\overline{X}_2}} > |\overline{X}_1 - \overline{X}_2|$$

The two means are considered different if:

$$\sqrt{S^2_{\overline{X}_1} + S^2_{\overline{X}_2}} < |\overline{X}_1 - \overline{X}_2|$$

This formula has been verified at the 5% limit by the t-test and was found to be conservative; therefore, it will be used in the discussion rather than the more tedious t-test.

A commonly used indication of the dispersion for a set of values is the Population Standard Deviation divided by the mean.

Dispersion = PSD/Mean

This measure of dispersion is also called the fractional standard deviation (FSD).

All grand correlation coefficients and grand dispersion indices are based on the grand abundances which are the mean abundances of the means for the large individual meteoritic fragments.

Comparison to Previous Work

The comparison of the Na and Mn abundances with independent determinations on different specimens agree very well with the work done by Schmitt et al. (30). Only the Na values of Holbrook and Leedey are higher in this work while the mean Na abundance of Atlanta is lower. The mean Na value of Leedey in this work has the same statistical mean as a flame photometry determination (34). The Mn range for Atlanta went from 540 ppm to 2060 ppm, which includes the value obtained by Schmitt (30). The other values are very nearly at the 5% confidence limit for the agreement between means (see Tables 37 and 38).

Table 37. Comparison of sodium abundance (ppm) from independent investigations.

Meteorite	This Study	INAA(30)	Distillation (8)	Flame Photo(34)
Richardton	5710 ± 304	5900 ± 580[a]	7100 ± 200	
Beardsley	5470 ± 269	5290 ± 100[a]	6600 ± 100	
Holbrook	7620 ± 42	6730 ± 140	7300 ± 100	
Leedey	7320 ± 490	6650 ± 130		7420
Bruderheim	6680 ± 236	6700 ± 290[b]		
Atlanta	3530 ± 997	4370 ± 80		

[a]Mean value of two specimens.

[b]Mean value of five specimens.

Table 38. Comparison of manganese abundance (ppm) from independent investigation.

Meteorite	This Study	INAA(30)	X-Ray Fluoresence (25)
Richardton (H)	2140 ± 82	2230 ± 50[a]	2400 ± 100
Beardsley (H)	2310 ± 39	2550 ± 350[a]	2500 ± 100
Holbrook (L)	2470 ± 50	2580 ± 80	2700 ± 100
Bruderheim (L)	2450 ± 64	2430 ± 120[b]	2700 ± 100
Covert (H)	2100 ± 193		2200 ± 100
Texline (H)	2310 ± 20		2400 ± 100
Leedey (L)	2580 ± 36	2440 ± 70	2700 ± 100
New Concord (L)	2500 ± 58		2800 ± 100
Potter (L)	2420 ± 112		3000 ± 100
Atlanta (E)	1170 ± 526	1770 ± 40	1570 ± 150

[a]Mean value of two specimens.

[b]Mean value of five specimens.

Table 39. Precision of determinations (ppm).

Meteorite and Specimen		Number of Individual Determinations I	II	III	Average value used in this paper
Leedey #1	Na	6610	6570		6590 ± 80
	Mn	2630	2620	2640	2630 ± 30
Plainview 92.995 #13	Na	5660	5640		5650 ± 85
	Mn	2250	2300		2280 ± 34
Miami #3	Na	5080	4980		5030 ± 76
	Mn	2070	1950	2070	2070 ± 25
Holbrook 75G #4	Na	7640	7600		7620 ± 115
	Mn	2330	2380	2340	2360 ± 35
Plainview 92EE #5	Na	5340	5610	5650	5630 ± 85
	Mn	2330	2290		2310 ± 25

The internal consistency and precision of the values obtained in this work are illustrated by showing the results of repeated abundance determinations for the same specimen in Table 39.

It is believed that this work has indicated that if appropriate care is taken, neutron activation analysis can be a precise analytical technique and the precision is also indicative of the accuracy of the method. It should be re-emphasized that even if there is a systematic error in this work, the values are consistent among themselves and the relative values are within the established error limits. Furthermore, any deviation resulting from equipment drift, flux variations, or error in the apparent half-lives will not be evident within a given set. As a result, the statements subsequently made concerning the homogeneity of the meteorites studied and consequential implications will be valid within the specified error limits. Since the specimens studied ranged from 0.5 to 1.2 grams, the conclusions subsequently made may not be valid for smaller specimens. If the volume of the individual crystals are large compared to the volume of the specimens, different specimens may be almost entirely composed of different types of crystals; therefore, the measurements on small specimens may not reflect the true homogeneity of the meteorite.

Homogeneity of Individual Meteorites

The Mn FSD for the two olivine bronzite falls ranged from 3.9% to 1.7% and the Na FSD ranged from 5.2% to 4.9%. The magnitude of the 3.9% Mn dispersion of the Beardsley chondrite arises primarily from specimen #3, which is four and one-half inches from specimen #1. (See Appendix for diagram). The Na dispersion in both chondrites is the result of no particular value, but represents a continuous range of abundances.

The first group of olivine bronzite finds (Tables 14, 21 and 22) had a Mn dispersion ranging from 0.8% to 2.7%, and a Na dispersion ranging from 1.8% to 4.7%. The large dispersion results primarily from one meteorite (Plainview 92.995). The abundances in the specimens of Plainview 92.995 causing the large dispersion were found to be consistant when reanalyzed and the dispersion should be considered real.

The second group of olivine bronzite finds (Tables 15, 23 and 24) show dispersion ranges of 3.8% to 16.9% for Mn and 3.8% to 30.8% for Na. The large dispersion of Mn results almost entirely from one specimen, #2, in the meteorite Channing 317.1x. The specimen was reanalyzed three times and the Mn abundance was accurately established at 1550 ppm which is 650 ppm lower than the highest Mn abundance found in specimen #3 which was separated by

only two inches. It may be significant to note that these two specimens were obtained from an edge which had been cut by a saw (see Appendix for diagram). There was also a significant Na depletion for specimen #2, although it was not as great as the Mn depletion. The largest Na dispersion is exhibited in specimen #2 of Covert 22Ax, which has a Na abundance of 5060 ppm which is significantly higher than the other specimens. This inhomogeneity is localized because specimen #2, which is very close to specimen #1, has an abundance in line with the other specimens.

The olivine hypersthene falls (Tables 16, 25 and 26) show an FSD ranging from 1.4% to 3.4% for Mn and 2.0% to 7.1% for Na. There is no single meteorite or specimen which can be pointed out as the cause of the Mn dispersion. The Na values are very homogeneous except for specimen #1 of Leedey 489.14x, which has a well established Na abundance significantly lower than the other specimens (see Appendix for diagram).

The olivine hypersthene finds (Tables 17, 27 and 28) showed a Mn dispersion ranging from 2.5% to 5.3% and a Na dispersion of 1.5% to 7.6%. There was a continuous range of abundances for both Mn and Na and no particular specimen or meteorite may be established as causing the dispersion.

The enstatite find was very inhomogeneous exhibiting marked differences in Mn and Na. The FSD's for the enstatite were 44.6%

for Mn and 28. 3% for Na.

When some of the marked variations are disregarded the homogeneity of a given meteorite follows roughly the dispersion indicative of the precision. The odd values of the finds may result from weathering and contamination. The odd values in the falls may result from contamination or by obtaining the major portion of a single large crystal in a specimen.

Schmitt et al. (30) using INAA determined the homogeneity of Na and Mn in three or more specimens of the same chondritic fall. For the olivine bronzite (H5) group their dispersion ranged from 3% to 7. 3%, and 4. 5% to 8. 7% for Mn and Na, respectively, in three or more specimens of the same meteorite. The author found for the same class of meteorites the dispersion was established to be 1. 7% to 3. 9% for Mn and 4. 9% to 5. 2% for Na in five or more specimens obtained from the same meteorite fragment. For the olivine hypersthene chondrites Schmitt et al. found the abundance dispersion for Mn in the same meteorites to be 2.9% to 4.9%; Na was 3% to 15%. This study found an abundance dispersion for five or more specimens of 1. 4% to 3. 4% for Mn and 2. 0% to 7. 1% for Na. The larger dispersion found by Schmitt et al. may be a combination of several factors. First, the precision of the previous work was not as high as the precision in this work. Second, in this paper the individual specimens came from a single large fragment while in Schmitt's work the

individual specimens may have come from different fragments in different meteorite collections. Third, the specimens studied by Schmitt et al. were considerably smaller than the specimens studied in this work. The specimen primarily responsible for the 15% Na dispersion for the hypersthene class in Schmitt's work had a mass of 91 mg. Therefore, the differences between the two studies are probably not in conflict.

Keil and Fredriksson (14) determined the homogeneity of Fe and Mg in individual crystals by using an electron microprobe. They found different olivine and pyroxene crystals or grains of a given chondrite vary less than ± 1% in their Fe/Mg ratio. This remarkable homogeneity in composition was observed in 86 of 95 chondrites studied. In the other chondrites the composition was found to vary by about ± 10%. Therefore, the homogeneity found by the author fits the general homogeneity pattern in ordinary chondrites as established by Keil and Fredriksson.

Homogeneity of Meteorite Classes

Olivine Bronzite Meteorites (H5)

Two olivine bronzite chondrite falls gave a weighted grand Na mean of 5590 ± 300 ppm with a PSD/mean of 0. 054 and Mn grand values of 2200 ± 117 ppm with a PSD/mean of 0. 052. However, the

Mn values for the two falls are distinctly different. The Richardton set has a mean Mn value of 2140 ± 83 ppm with a PSD/mean of 0.039 while the Beardsley set has a Mn mean of 2310 ± 39 ppm for a PSD/mean of 0.017.

It was also discovered that olivine bronzite finds could be grouped into two similar distinct groups on the basis of the Mn abundances and population dispersion. Group A, consisting of four Plainviews and Texline, had a mean Mn abundance of 2320 ± 56 ppm with a PSD/mean of 0.024. The Na abundance of Group A was 5660 ± 256 ppm with a PSD/mean of 0.045. Therefore, it appears that Beardsley, a fall, belongs to Group A. Group B finds consisting of Channing, Covert, Acme and Miami, had a grand Mn mean of 2040 ± 175 ppm with a PSD/mean of 0.085, and Na abundances of 4220 ± 778 ppm with a PSD/mean of 0.184. It, therefore, appears that on the basis of the Mn abundances and the Mn PSD/mean values Richardton belongs with the Group B finds.

To summarize the reasons for classifying the H5 meteorites into two classes

1. The Mn means for Group A and Group B are distinclty different at the 5% level.

2. The homogeneity of the Mn for Group A is much greater than the homogeneity of Group B.

$$\frac{\text{PSD/mean (Group A)}}{\text{PSD/mean (Group B)}} \approx 0.28$$

3. The Na abundances for Group A finds are about 25% higher than the abundance of Group B finds and for the finds the Na dispersion was significantly different.

$$\frac{\text{PSD/mean (Group A)}}{\text{PSD/mean (Group B)}} \approx 0.25$$

It should be noted, however, that no such effects for sodium were realized for the falls. It is, therefore, possible that effects observed for Na and Mn arise for different reasons.

Olivine Hypersthene (L6) and Enstatites (E5)

No significant subgrouping of the L6 chondrites were established in this study as was suggested for the H5 group.

The hypersthene chondritic falls exhibited a grand mean of 2470 ± 85 ppm Mn with a PSD/mean of 0.034. The grand mean Na value for the falls was 7360 ± 547 ppm with a PSD/mean of 0.072. The inverse square weighted abundances of the olivine hypersthene finds showed a grand mean of 2420 ± 97 ppm with a PSD/mean of 0.040 and 6060 ± 370 ppm with a PSD/mean of 0.061 for Mn and Na, respectively.

Only one enstatite, a find, was analyzed. It was very inhomogeneous giving a mean of 1170 ± 526 ppm with a PSD/mean of 0.446 and 3530 ± 997 ppm with a PSD/mean of 0.283 for Mn and

Na, respectively.

Evidence for Metamorphism

Richardton exhibits a Mn abundance of 2140 ± 83 ppm and a Na abundance of 5710 ± 304 ppm with a Mn dispersion of 3.9% and a Na dispersion of 5.2%. Beardsley was found to show a Mn abundance of 2310 ± 39 ppm with a dispersion of 1.7% and a Na abundance of 5470 ± 269 ppm with a dispersion of 4.9%.

The differences in Mn abundance and dispersion between Richardton and Beardsley may be indicative of a metamorphic process. This idea arises by considering the connection between Xe^{129} ages and the Mn - Na abundance pattern. Richardton began to retain Xe^{129} about 50 ± 60 my.after t_o; however, the more recrystallized Beardsley did not retain Xe^{129} until 100 - 200 my. later. This perhaps indicates an origin in a deeper location or in a larger parent body (3). Mn^{++} presumably diffuses much slower than Na^{+} (22) in a metamorphic process. Therefore, Na would tend to be more homogeneous throughout the entire body than Mn, and would be slightly more homogeneous for fragments of the parent body which experienced a greater metamorphism. Mn would be expected to be less homogeneous throughout the entire parent body since it does not diffuse as rapidly as Na. Furthermore, between two fragments of the parent body, the fragment originating from the interior, having

experienced greater metamorphism, would be expected to be more homogeneous than a fragment originating from the exterior edge of the parent body. This is what was observed for Richardton and Beardsley suggesting evidence for metamorphic fractionation in the parent body of meteorites.

In addition, if Mn and Na were correlated in the original condensation from the primitive solar nebula as postulated by Larimer (15) and Larimer and Anders (16), a fragment of the parent body which had not undergone a high degree of change via metamorphism should reflect this correlation. Richardton exhibits a correlation coefficient of 0.91. If another sample underwent metamorphism the correlation would be destroyed because the more mobile Na^{+} ion migrates more rapidly than the firmly held Mn^{++} ions. The more highly metamorphisized Beardsley exhibits this feature by having a correlation coefficient of -0.51.

Distribution Implications In Individual Meteorites

It is difficult to definitely establish a distribution gradient in a given fragment. Certainly no obvious gradient is indicated by the data for Na; however, for certain of the falls a Mn concentration gradient is implied. Further investigation is necessary to ascertain if such gradients are real. Such investigations could be carried out by drilling a core in the direction of the implied gradient and

analyzing small segments of the core.

Bruderheim (L6) appears to have a vertical gradient of about 20 ppm/inch. A diagram of Bruderheim is given in the Appendix. A schematic vertical diagram is given below.

Table 40. Abundance gradient of Bruderheim.

Height above base	Specimen number	Mn ppm
5 1/2"	3	2550 ± 38
2 3/4"	2	2500 ± 38
1/2"	4	2440 ± 25

Specimens #1 and #5 were within one-half inch vertically of specimen #4 and all three values were statistically the same. Specimens #3 and #2 have a 36% chance of being different by applying the standard statistical test (26)

$$Z = (X_1 - X_2)/\sqrt{\sigma_1^2/N_1 + \sigma_2^2/N_2}.$$

Leedey (L6) may also indicate a concentration gradient in the plane consisting of specimens 1, 5, and 3.

Table 41. Abundance gradient of Leedey.

Specimen #	Distance from Specimen #1 (inches)	Abundance (ppm)	Gradient
1		2630 ± 30	
5	2	2590 ± 39	20 ppm/inch
3	4	2550 ± 38	20 ppm/inch

The approximate gradient between positions #5 and #3 is about 20 ppm/inch. The difference between 1 and 3 may be considered real with 95% certainty and the difference between 1 and 5 may be considered a real difference about 42% of the time.

Admittedly no conclusion can be drawn as to the existence of a concentration gradient. However, since this was the first relatively complete study on the homogeneity of chondritic meteorites with high degree of precision, it was felt that this point should be alluded to as a project for further investigation. If such a gradient is later established it may be related to a concentration gradient in the primitive solar nebula, or it may be related to metamorphic processes in the parent body.

The apparent FSD differences in Group A and Group B of olivine bronzite (H5) class, as well as intergroup FSD differences, may be related to the homogeneity of the original solar nebula. If this is the case, it implies that the parent bodies may have accreted from different regions of the nebula. However, as mentioned before

metamorphism may have played a significant part in the homogenization and fractionation of many meteorites.

On the basis of 1000 atoms/cm^3 (11) and 1% accretion of available material (7), a 1 kg fragment would have required about 10^8 - 10^9 km^3 of primitive solar dust to form. This emphasizes the degree of homogeneity that the solar nebula must have had before accretion.

Table 42. Intergroup comparisons.

Class	Mn (ppm)	PSD/mean	Na (ppm)	PSD/mean
Olivine Bronzite H5	2200 ± 117	0.052	5590 ± 300	0.054
Olivine Hypersthene L6	2470 ± 85	0.034	7360 ± 547	0.074
Enstatite E5	1170 ± 526	0.446	4130 ± 757	0.183

From the above table it appears that each of the three classes are distinct on the basis of Na and Mn abundances. In addition, to the distinct grouping by abundances the population dispersions also tend to suggest classifications.

Manganese and Sodium Correlation

The grand correlation coefficients of each of the sets and groups were determined and are reported in Table 43.

Table 43. Grand correlation coefficients.

Class	Correlation coefficient (weighted)
Olivine Bronzite (H5) falls	-0. 10
Olivine Bronzite (H5) finds	
Group A	+0. 73
Group B	+0. 28
Hypersthene (L6) falls	-0. 29
Hypersthene (L6) finds	-0. 22
Enstatite (E5) finds	+0. 38

Intergroup Comparisons

For the intergroup comparisons only the limited number of falls analyzed and the enstatite find are considered so that the effects of complicated terrestrial processes, such as weathering, are minimal.

The interpretation of these values presents a difficult problem because some of the individual sets have high correlation coefficients both positive and negative. Without the Xe^{129} ages, which were available for Richardton and Beardsley, no significant correlations can be established for falls. For finds weathering has altered the correlation so no significant relations can be established for them. In some cases the error assigned to values are sufficiently large so that two values for the same specimen which are within one standard

deviation would be sufficient to change an inverse correlation to a positive correlation. Therefore, it was concluded that no significant correlation between Mn and Na was generally established. Schmitt et al. (30) established correlation coefficients of +0.43 for the H group (olivine bronzites), +0.61 for the L group (olivine-hypersthene) and + 0.68 for the enstatite class studied here and concluded that the correlation was not significant.

Both in Schmitt's work and the author's work no significant correlation was established, as implied by Larimer (10, 11), between sodium and manganese. It is possible that a correlation did exist at one time, but was altered by later processes. Also the degree of correlation may not be as significant as expected.

Terrestrial Fractionation

If it is assumed that the olivine hypersthene chondrites have a unique Mn and Na content, a major fractionation process due to terrestrial leaching by water may be inferred from the abundance and the FSD values of Na and Mn. This is illustrated by considering grand weighted mean values of Mn and Na for the olivine hypersthene chondrites.

Table 44. Evidence of leaching.

Element	Fall (ppm)	Find (ppm)	Find/fall
Mn	2470	2420	0.94
Na	7360	6060	0.82

Table 45. Average increase in dispersion due to possible weathering.

Element	Fall	Find	Find/fall
Mn	0.020	0.041	2.0
Na	0.031	0.049	1.6

These values follow the general trend expected for a leaching process, namely, a lowering of the absolute abundances and an increase in the dispersion of the values for the weathered samples. The general trend of increased dispersion and decreased abundances, although not so evident in this study for olivine bronzites, is substantiated in other work (25, 30). Moore and Brown (23) using spectrographic method did not observe a significant Mn depletion.

An excellent example of the inhomogeneity introduced by weathering is evidenced in Potter 476.67 (see diagram in Appendix) which shows extreme weathering effects. The Mn values are more consistent than the wide range of values for Na which shows severe depletion. Specimens which are close together may show extreme variation; for example, positions #1 and #2 were separated by about

1.5 inches and the sodium values changed by 26%. Extreme variations in abundances are a common geochemical phenomena and are dependent upon the minerals which the element forms, the degree of porosity of the meteorite and mineral content of meteoritic environment. It is even possible for an enrichment of an element to occur (23). The magnitude of the weathering effects are dependent on the terrestrial age. Potter which shows extreme weathering has a terrestrial age > 20, 000 years while Plainview which does not exhibit weathering effects has a terrestrial age < 2000 years (2). Therefore, great care must be taken in correlating data for finds to initial processes which occurred in meteorites.

Sampling Errors

This study has indicated that significant inhomogeneity errors should not be a major factor in the determination of Na and Mn abundance values for falls of several kilograms in mass. A few grams may be considered as a representative sample within ± 6% of the mean abundance value for olivine bronzite and olivine hypersthene chondrites. When determining Na and Mn abundances in these meteorite classes it is not necessary to sample as extensively as had been previously suggested (14). Greater care must be taken when considering finds since weathering may have caused significant inhomogeneities, especially with Na. Since Na and Mn were found to be very inhomogeneous in the enstatite chondrite, one specimen does not adequately represent the Na and Mn abundances.

SUMMARY AND CONCLUSION

Twenty-three meteorite fragments representing both finds and falls for the olivine bronzite, olivine hypersthene and enstatite classes were sampled in five positions. The manganese and sodium abundances for each specimen were determined to a precision of ± 1.5% via instrumental neutron activation analysis using the photopeak area method. A three by three inch NaI (Tl) detector coupled to a 400 channel analyzer was used in detecting the gamma radiation of the specimens. The Mn 0.84 Mev photopeak and the Na 2.75 Mev photopeak were used in the determinations.

The olivine bronzite falls (H5) were found to exhibit a Mn homogeneity of 3.9% to 1.7% for the large individual meteorites; Na dispersion was 5.2% to 4.9%. One group of olivine bronzite (H5) finds consisting of five large meteorite fragments exhibited a Mn dispersion of 0.8% to 2.7%; Na disperions was 1.8% to 4.7%. Another group of olivine bronzite (H5) finds consisting of four individual pieces showed a Mn dispersion range of 3.8% to 16.9%; Na dispersion ran from 3.8% to 30.8%. The olivine hypersthene (L6) falls showed a Mn dispersion of 1.4% to 3.4%; Na dispersion ranged from 2.0% to 7.1%. The olivine hypersthene finds showed a Mn dispersion of 2.5% to 5.3%; Na dispersion was 1.5% to 7.6%. The single enstatite find showed an FSD of 45% for Mn and 28% for Na.

The olivine bronzite (H5) chondrites were found to represent two distinct groups on the basis of Mn abundances and FSD. The tentative classification was based on only a limited number of meteorites: one group consisted of three meteorites (six large fragments) and a second group consisted of five meteorites (five large fragments). It is suggested that the two falls analyzed which apparently belong to different olivine bronzite (H5) subgroups are partially the result of a metamorphic process in the parent body.

The results of the analysis of the falls for all classes are given below including the single enstatite find analyzed.

Table 46. Abundances and dispersion of meteorite classes.

Class	Mn (ppm)	Mn FSD	Na (ppm)	Na FSD
Olivine Bronzite (H5)				
Group A	2310 ± 39	0.017	5470 ± 269	0.049
Group B	2140 ± 83	0.038	5740 ± 304	0.052
Olivine Hypersthene (L6)	2470 ± 85	0.035	7360 ± 547	0.074
Enstatite (E5)	1170 ± 526	0.446	4130 ± 757	0.183

The differences in the mean abundance values between each class are significant except for the sodium values of the olivine bronzite Group A and B.

No significant correlation between Na and Mn was established as was implied in previous theoretical work (15, 16). Previous

work (30) also found no correlation between these elements. It is suggested that if a correlation between Na and Mn did exist, it may have been destroyed by metamorphism.

It was found that terrestrial fractionation apparently occurred in the finds resulting from weathering of the chondrites. It was suggested that significant depletion of Na may occur but Mn depletion is not as pronounced in weathered finds. Furthermore, a significant decrease in homogeneity apparently results from weathering, increasing both the FSD of Mn and Na by a factor of about two for finds compared to the FSD of falls.

It is suggested that for certain olivine-hypersthene falls a concentration gradient may be present. The gradient is not confirmed but mentioned as a point for further investigation.

It is the hope of the author that this study has shown that INAA is an effective and highly precise analytical technique and further investigation as to the homogeneity of meteorites may result in useful and pertinent information as to the origin of meteorites and perhaps in turn, information about the early history of our solar system.

BIBLIOGRAPHY

1. Anders, Edward. Chemical fractionation in meteorites. Meteoritika 26:17-25. 1965.

2. Anders, Edward. Meteorite ages. Reviews of Modern Physics 34:287-325. 1962.

3. Anders, Edward. Origin, age, and composition of meteorites. Space Science Reviews 3:583-714. 1964.

4. Bleuler, Ernst and George J. Goldsmith. Experimental nucleonics. New York, Holt, Rhinehart and Winston, 1963. 393 p.

5. Bowen, H. J. M. and D. Gibbons. Radioactivation analysis. Oxford, Clarendon Press, 1963. 295 p.

6. Cameron, A. G. W. The accumulation of chondritic material. Earth and Planetary Letters 1:93-96. 1966.

7. Cameron, A. G. W. The collapse phase of early solar evolution. Washington, D. C. 11 P. (U. S. National Aeronautics and Space Administration. Technical Note D no. 1682)

8. Edwards, George and Harold C. Urey. Determination of alkali metals in meteorites by a distillation process. Geochimica et Cosmochimica Acta 7:154-168. 1955.

9. Fish, Robert A., Gordon G. Goles and Edward Anders. The record in the meteorites. III. On the development of meteorites in asteroidal bodies. Journal of Astrophysics 66:1509-1511. 1961.

10. Freidlander, G., J. W. Kennedey and J. M. Miller. Nuclear and radiochemistry. 2d ed. New York, John Wiley and Sons, 1964. 585 p.

11. Goldschmidt, V. M. Geochemistry. Oxford, Clarendon Press, 1954. 912 p.

12. Hey, Max H. Catalogue of meteorites. 3d ed. Oxford, Alden Press, 1966. 637 p.

13. Krinov, E. L. Principles of meteoritics. New York, Pergamon Press, 1960. 535 p.

14. Keil, Klaus. The iron, magnesium, and calcium distribution in coexisting olivines and rhombic pyroxenes of chondrites. Journal of Geophysical Research 69:3487-3515.

15. Larimer, John W. Chemical fractionations in meteorites - I. Condensation of the elements. Geochimica et Cosmochimica Acta 31:1215-1238. 1967.

16. Larimer, John W. and Edward Anders. Chemical fractionations in meteorites - II. Abundance patterns and their interpretation. Geochimica et Cosmochimica Acta 31:1239-1270. 1967.

17. Lenihan, J. M. A. and S. J. Thomson. Activation analysis principles and applications. London, Academic Press, 1965. 211 p.

18. Linn, T. A. The concentrations and distributions of selected chemical elements in the metallic, sulfide and phosphide phases of iron meteorites via neutron activation analysis. Ph. D. thesis. Tempe, Arizona State University, 1967. 143 numb. leaves.

19. Mason, Brian. The chemical composition of olivine-bronzite and olivine-hypersthene chondrites. American Museum of Natural History, American Museum Novitates no. 2223. 38 p. 1965.

20. Mason, Brian. Geochemistry and meteorites. Geochimica et Cosmochimica Acta 30:365-374. 1966.

21. Mason, Brian. Meteorites. New York, John Wiley and Sons, 1962. 274 p.

22. Mason, Brian. Principles of geochemistry. 2d ed. New York, John Wiley and Sons, 1965. 310 p.

23. Moore, Carleton B. and H. Brown. The distribution of manganese and titanium in stony meteorites. Geochimica et Cosmochimica Acta 26:495-502. 1962.

24. Moore, Carleton B. and Charles F. Lewis. Catalog of meteorites in the collections of Arizona State University. Tempe, Arizona State University, 1964. 1302 p.

25. Nichiporuk, Walter, A. Chodos, E. Helin and H. Brown. Determination of iron, nickel, cobalt, calcium, chromium and manganese in stoney meteorites by X-ray fluorescence. Geochimica et Cosmochimica Acta 31:1911-1930. 1967.

26. Parrat, Lyman G. Probability and experimental errors in science. New York, John Wiley and Sons, 1961. 255 p.

27. Ringwood, A. E. Chemical and genetic relationships among meteorites. Geochimica et Cosmochimica Acta 24:159-197. 1961.

28. Reynolds, J. H. Isotopic abundance anomalies in the solar system. Annual Review of Nuclear Science 17:253-316. 1967.

29. Schmitt, R. A., G. G. Goles and R. A. Smith. Abundances of Na, Sc, Cr, Mn, Fe, Co and Cu in 92 meteorites, 9 terrestrial specimens and 90 individual chondrules. San Diego, Calif. General Atomic, 1963. 42 p. (GA-4782)

30. Schmitt, R. A., G. G. Goles and R. H. Smith. Elemental abundances in stone meteorites. (in preparation)

31. Schmitt, R. A., R. H. Smith and G. G. Goles. Abundances of Na, Sc, Cr, Mn, Fe, Co, and Cu in 218 individual chondrules via activation analysis. I. Journal of Geophysical Research 70:2419-2444. 1965.

32. Suess, Hans E. Metamorphosis and equilibration in chondrites. Journal of Geophysical Research 72:3609-3612. 1967.

33. Upham, Gary. Flux measurements in the Oregon State TRIGA Reactor. M. S. thesis. Corvallis, Oregon State University, 1968. 105 numb. leaves.

34. Urey, Harold C. A review of atomic abundances in chondrites and the origin of meteorites. Reviews of Geophysics 2:1-34. 1964.

35. Urey, Harold C. and Harmon Craig. The composition of the stone meteorites and the origin of the meteorites. Geochimica et Cosmochimica Acta 4:36-82. 1953.

36. Van Schmus, W. R. and J. A. Wood. A chemical-petrologic classification for chondritic meteorites. Geochimica et Cosmochimica Acta 31:747-765. 1967.

37. Whipple, Fred L. The history of the solar system. Proceeding of the National Academy of Sciences 52:565-594. 1964.

38. Wood, John A. Chondrites and chondrules. Scientific American 209:64-82. 1963.

39. Wood, John A., Physics and chemistry of meteorites. The Solar System 4:377-401. 1963.

40. Wood, John A. and A. C. W. Cameron. On the origin of chondrules and chondrites. Icarus 2:152-180. 1963.

APPENDIX

Position of Specimens on Selected Meteorites

On the following diagrams the positions of the specimens are numbered. The position of the specimen above the base of the meteorite is indicated by H + X, where X is the distance of the base. All distances are in inches.

Olivine Bronzite - Falls

Meteorite

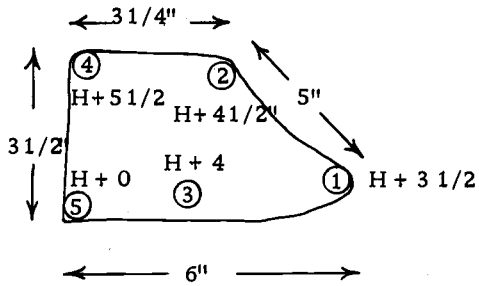

Description

Richardton 100H (H5)
Olivine Bronzite - Fall
5775 grams

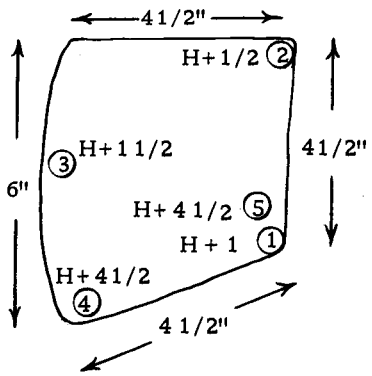

Beardsley 134 AX (H5)
Olivine Bronzite - Fall
4401.8 grams
Specimens 1 and 5 separated vertically by 3 1/2" and 1" horizontally.

Olivine Bronzite - Finds

Meteorite

Description

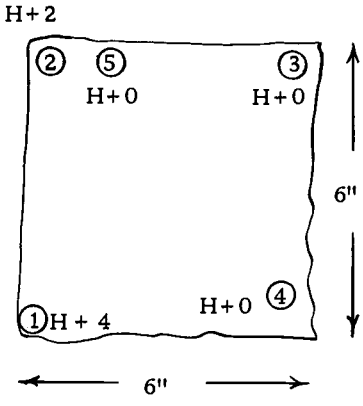

Plainview 92.995
Olivine Bronzite (H5)
Find
4983 grams

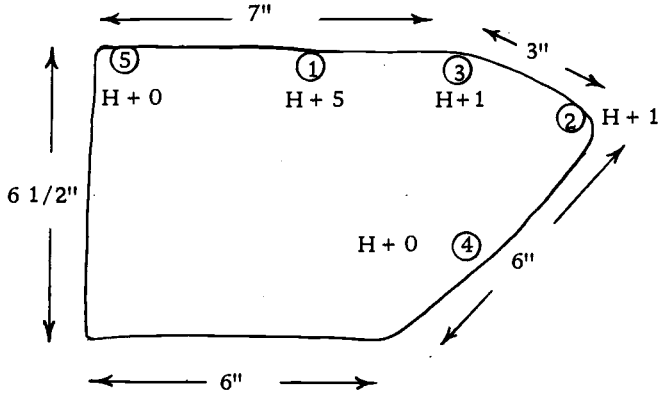

Plainview 92F
Olivine Bronzite (H5)
Find
8833 grams

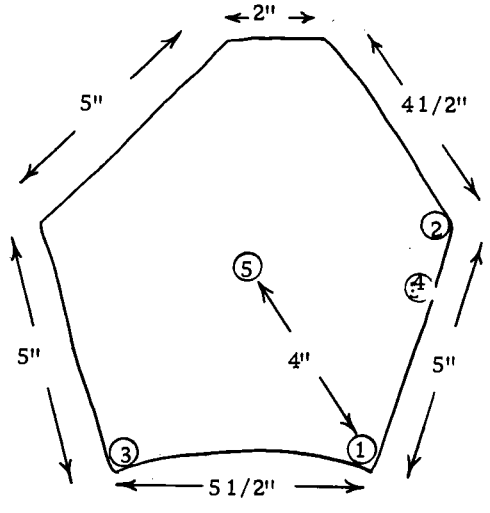

Texline 415.1X
Olivine Bronzite (H5)
Find
7455.7 grams

Olivine Bronzite - Finds

Meteorite

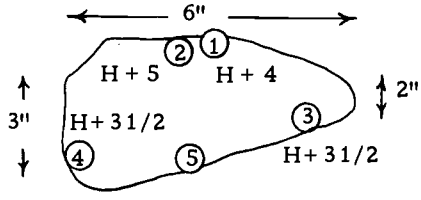

Description

Covert 22AX
Olivine Bronzite - (H5)
Find
3629 grams
Specimens 1 and 2 are separated by 1" vertically and 1 1/2" horizontally

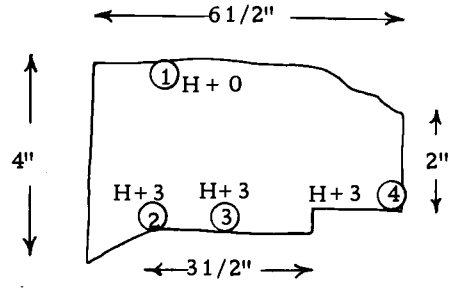

Channing 317. 1X
Olivine Bronzite (H5)
Find
2538. 7 grams
Specimens 2, 3 and 4 lie along side cut by a saw.

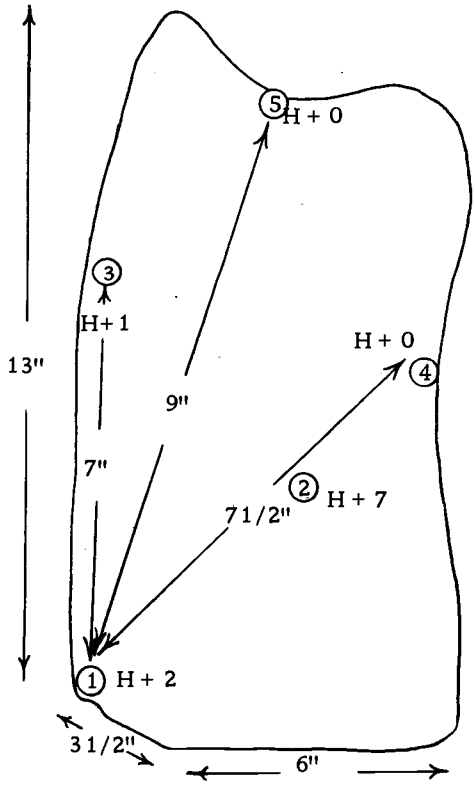

Maimi 399. 1X
Olivine Bronzite (H5)
Find
29, 024 grams

Olivine Hypersthene - Falls

Meteorite

Description

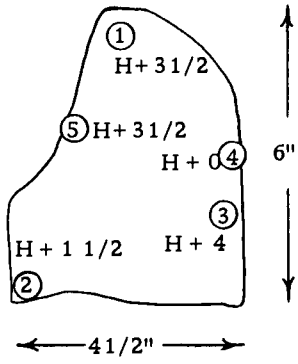

Leedey 489.1
Hypersthene (L6)
Fall
6123.6 grams

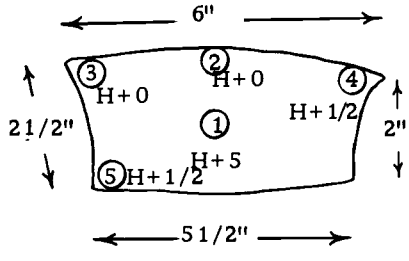

Holbrook 57G
Hypersthene (L6)
Fall
2491 grams

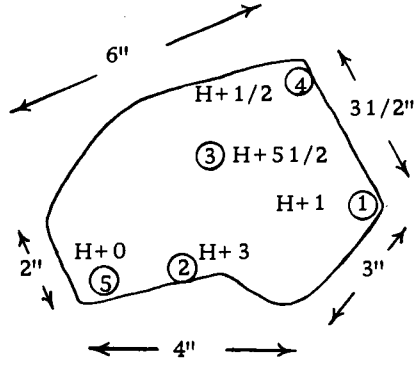

Bruderheim 705
Hypersthene (L6)
Fall
3880 grams

Olivine Hypersthene - Finds

Meteorite

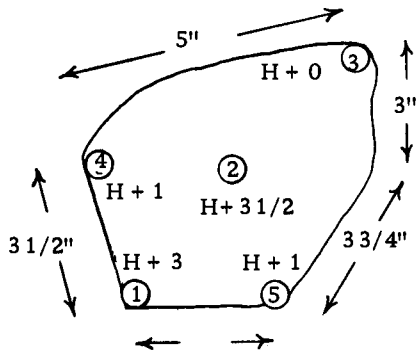

Description

Ladder Creek 405 hx
Hypersthene (L6)
Find
5385 grams

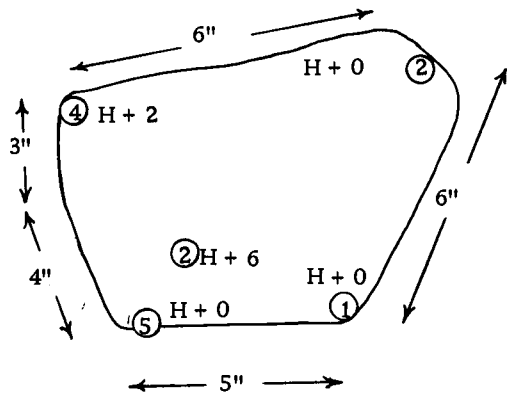

Harrisonville 174. 24
Hypersthene (L6)
Find
6879 grams

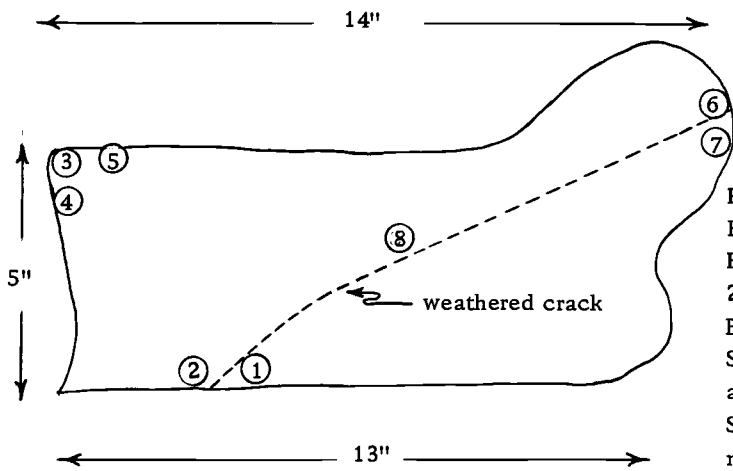

Potter 476. 67
Hypersthene (L6)
Find
23556 grams
Badly weathered
Specimens 1, 2, 6, 7, and 8 taken along weathered crack.
Specimens 4, 5, 3 taken from more solid portion.